Developing Cell Quenching Method to Facilitate Single Cell Mass Spectrometry Metabolomics Studies

Shakya Wije Munige[#a], Deepti Bhusal[#a], Zongkai Peng[a], Dan Chen[a], Zhibo Yang[*a,b]

[a] Department of Chemistry and Biochemistry, University of Oklahoma, Norman, Oklahoma, 73019, US

[b] Stephenson Cancer Center, University of Oklahoma Health Sciences Center, Oklahoma City, Oklahoma, 73104, US

[#]These authors contributed equally

[*] Corresponding author

[*]Zhibo.Yang@ou.edu

ABSTRACT: Single-cell mass spectrometry (SCMS) has emerged as a powerful tool for analyzing metabolites in individual cells, including live cells. However, cell metabolites have rapid turnover rate, whereas maintaining metabolites' profiles of live cells during sample transport, storage, or extended measurements can be challenging. In this study, a cell preparation method, which integrates cell washing by nonvolatile salt solution, rapid liquid nitrogen (LN_2) quenching, freeze-drying in vacuum, and freezer storage at -80 °C, to preserve cell metabolites for SCMS measurement. Experimental results revealed that LN_2 quenching preserved the overall cell metabolome, whereas storage at -80 °C for 48 h slightly changed metabolites' profiles in quenched cells. However, metabolites in unquenched cells were changed regardless of low-temperature storage. The influence of omission of quenching and low-temperature storage on cell metabolites and relevant pathways were investigated. Results from this work indicate that cell quenching is necessary, but low-temperature storage time should be minimized to preserve cell metabolites. The method developed in the current work can be readily adopted by SCMS techniques storage remained largely unaltered, allowing for extended SCMS studies.

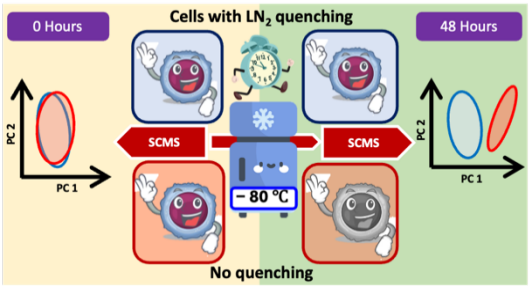

INTRODUCTION

The ability to detect cell-to-cell variation allows for the discovery of hidden mechanisms that may be intractable to studies using bulk samples.[1] Single-cell analysis has become a powerful tool in biological research, enabling a deeper understanding of the complexity and heterogeneity inherent in biological systems. This approach allows for studying unique characteristics, such as gene expression, protein levels, metabolomic features, and cellular behavior, at cellular level. Single-cell analysis enables us to identify rare cell populations and subpopulations with unique functions or characteristics. Single cell analysis has revolutionized research in numerous files, opening new avenues for discovery and advancing our understanding of life at the single-cell level.[2] Such analysis unveils crucial insights into multiple aspects, such as developmental processes, disease progression, and therapeutic responses, in studies of disease mechanisms and personalized treatment.

The area of single-cell analysis presents multiple challenges, including very limited sample amounts (e.g., the volume of a typical mammalian cell ranges between 1 and 10 pL)[3-5] and extremely complex compositions (e.g., ~2-4 million proteins/μm^3 and >42,000 metabolites in a cell)[6, 7]. Omics endeavors to thoroughly characterize all elements of cellular systems. Numerous cutting-edge technologies have been employed to study genomics[8], epigenomics[9], transcriptomics[10], proteomics[11], and metabolomics[12] at the single-cell level. The metabolome, encompassing the entirety of a cell's metabolites, emerges as a sensitive response to cell status and alterations in its surroundings. Unlike genes and proteins, which represent the cell's potential capabilities, the metabolome has more rapid (e.g., within a few seconds) response to environmental perturbations[13, 14]. Studying the metabolome provides a unique lens into the immediate impact of environmental changes on the cell's functional state, offering insights that extend beyond the capabilities of genomic and proteomic analyses. Thus, in addition to above-stated challenges (i.e., extremely limited sample amount and complex compositions), metabolomics studies of single cells, particularly for cells in their living status, need to minimize the influence of rapid turnover rates on profiles of cell metabolites during data acquisition.[15]

Multiple techniques, including nuclear magnetic resonance (NMR) spectroscopy, fluorescence microscopy[16, 17] , and mass spectrometry (MS), are commonly used for conventional metabolomics studies. Among them, MS-based methods are more effective for single cell metabolomic analysis due to its unique advantages: highly sensitive for detection and highly accurate for identification of extremely low abundance molecules with complex compositions[2, 18]. Several types of single-cell MS (SCMS) methods, categorized as either vacuum-

based or ambient-based techniques, according to their sampling and ionization conditions, have been created and utilized for examining various cell types, including plant cells, mammalian cells, and yeasts.[15, 19-22] Vacuum-based SCMS methods predominantly rely on two approaches: secondary ion mass spectrometry (SIMS) and matrix-assisted desorption/ionization (MALDI) mass spectrometry. These techniques employ high-energy ion beams (for SIMS) or ultraviolet (UV) laser pulses (for MALDI-MS) to desorb and ionize cellular molecules, including metabolites, lipids, and pharmaceuticals, enabling sensitive and consistent analysis at the individual cell level.[19, 23] Unlike vacuum-based methods, ambient SCMS techniques enable analysis of cells with minimal or no sample preparation[24, 25]. Various ambient SCMS methods have been developed, including laser ablation electrospray ionization (LAESI) MS[26], live single-cell video-MS, induced nanoESI (InESI) MS[27], nano-spray desorption electrospray ionization (nano-DESI) MS[28], probe electrospray ionization (PESI)[29, 30], and methods integrated with microfluidic chips[31-33] and flow cytometry[34]. We have developed the Single-probe, a multifunctional device that can be coupled to MS for single cell studies[35, 36], MS imaging of tissues[36, 37], and analysis of extracellular molecules within live spheroids[38] in ambient environment. In addition, we have created the T-probe[39, 40] and micropipette capillary[41] for SCMS measurements. These methodologies offer significant potential for exploring basic cell biology (e.g., cell heterogeneity[42-44], cell-cell interactions[16], and influence of environment on cell metabolism[45, 46]) and potential clinical applications (e.g., quantification of drug[47] and signaling molecules in single cells[48, 49], drug resistance[36, 50, 51], and drug influence on cell metabolism[48, 50, 52]). Among them, the Single-probe SCMS technique is routinely used for our SCMS metabolomics studies of live cells.

Although most ambient-based SCMS techniques allow for the analysis of live cells, they generally have relatively low throughput (e.g., 15 cells from nano-DESI MS[28], 32 cells from microprobe Capillary electrophoresis (CE)-ESI-MS[53], and 108 cells from the Single-probe SCMS[36]), largely due to necessary manual selection and analysis of individual cells. Because of the dynamic nature of cell metabolism, cell metabolites may vary during lengthy sample preparation and measurement. To preserve metabolomics features of live cells, researchers used quenching methods after cell isolation[5, 54]. Quenching can stop cellular metabolism and metabolomic transformations[55] by lowing temperature[56] (e.g., using liquid nitrogen (LN_2) for snap freezing)[57, 58] or denaturing enzymes[59] (e.g., adding organic solvents or acidic solutions)[57, 60, 61] of cells. Quenching is pivotal to effectively arresting the cells' metabolic activities, encapsulating a momentary freeze-frame of its biochemical state[62]. This is crucial for accurate metabolomic studies, in which capturing the precise temporal details of cellular metabolites is essential for understanding cellular function.

An effective protocol for quenching should take certain factors into consideration to achieve rapid and thorough inhibition of intracellular metabolic reactions[58]. Studies have been performed to evaluate the performance of different quenching protocols, including cold isotonic saline (0.9% NaCl)[63], chilled acetonitrile (at -40°C)[60], cold methanol (60%, at -40°C) containing buffer salts (e.g., ammonium bicarbonate[61], NaCl[58, 61, 63], HEPES[61, 64], ammonium carbonate[64]), ice-cold phosphate-buffered saline (PBS)[57, 65], LN_2[57, 58, 66], and hot air treatments[67]. In fact, some of these above quenching methods were designed for MS metabolomics studies of bulk cell samples,[58, 60, 63, 65] and cold methanol and acetonitrile have been utilized with Pico-ESI-MS[5] and MALDI-MS techniques,[60] respectively, for in single cell studies. Although these quenching methods have demonstrated their efficacy in halting enzymatic activity and preserving cellular metabolites, each approach has its own limitations: organic solvents could lead to metabolite leakage and cell membrane damage[63, 68]; using solutions containing nonvolatile salts can severely impact MS analysis due to matrix effect,[60] which leads to ion suppression[69], reduced sensitivity, inaccurate quantification of analytes,[61, 70] and ion signal interference.

LN_2 snap freezing has been widely used in biological research[71]. Instead of using cold organic solvents containing buffer salts, quenching by LN_2 seems more suitable for SCMS studies because LN_2 can immediately stop metabolomic activities without leaving residual nonvolatile salts after LN_2 evaporation. However, previous studies showed LN_2 snap freezing often led to cell membrane damage[72, 73], which is undesirable for SCMS studies. To prevent cell membrane damage in LN_2 quenching, a method combining fast filtration, NaCl solution washing, and LN_2 freezing was employed for the metabolome analysis of suspended animal cells[62, 68]. Briefly, cell suspension was quickly filtered by a filter (glass fiber filter disk) using a vacuum, and the filter containing cells was rinsed by cold iso-osmotic NaCl solution to remove residual culture medium and then frozen in LN_2. This method is effective to retain metabolites, including those with high turnover rates, and mitigate cell membrane damage,[62, 68] but it is unlikely suitable for SCMS studies because of challenges to isolate cells for experiment and matrix effect due to remaining nonvolatile salts. In addition to LN_2 quenching, sample storage in a -80 °C freezer is commonly used to preserve cells and tissues prior to analysis. However, the influence of storage at -80 °C on metabolite profiles of single cells has not been previously reported. There is a crucial need for developing new cell quenching methods for robust SCMS metabolomics studies.

In the current work, we developed a new protocol, which combines cell washing by nonvolatile salt solution, LN_2 quenching, freeze drying in vacuum, and low-temperature storage, for sensitive ambient SCMS analysis. An advantage of our method is to incorporate a rapid washing[66] utilizing the solution containing ammonium formate (AF), which is compatible with live cells and MS analysis[5], prior to rapid LN_2 quenching to minimize cell membrane damage. Quenched cells are then rapidly dried in a vacuum with the presence of residual LN_2 to efficiently remove water molecules from cells, allowing for minimized metabolic activities and degradation of metabolites of cells during SCMS measurement in ambient environment. We also evaluated the influence of storage in a -80 °C freezer on cells' metabolites. Our methods can be readily adopted by researchers for robust SCMS metabolomics studies using other types of techniques.

EXPERIMENTAL SECTION

Cell culture

HCT-116 cells were grown in McCoy's 5A Medium (Fisher Scientific Company LLC, IL, USA) supplemented with 10% fetal bovine serum (FBS, GE Healthcare Bio-science Corp, Marlborough, MA, USA) and 1% penicillin-streptomycin (Life Technologies Corporation, Grand Island, NY, USA). Cells were cultured in an incubator (HeraCell, Heraeus, Germany) at 37°C in presence of 5% CO_2. Cells were passaged every two days when their confluence reached 80%. To perform cell

passaging, 2 mL of trypsin-EDTA (Life Technologies Corporation, Grand Island, NY, USA) was introduced into a petri dish and incubated at 37°C for 3 minutes to detach the cells. Following this, 8 mL of cell culture medium was added to deactivate the trypsin enzymatic activity. Subculturing was carried out by transferring 1 mL of the cell suspension solution into 9 mL of fresh culture medium.

Cell seeding was performed using cell suspension solution (~1x10^6 cells/mL) in culture medium. For experimental replication, four glass coverslips (18 mm, VMR micro cover glass, USA. CAT. No. 48380046) were individually placed in four wells of a 12-well plate. An aliquot of 2 mL/well of cell culture media was transferred to these four wells, and 200 µL (~2x10^5 cells/well) of cell suspension solution was added into each well containing a coverslip. The prepared 12-well plate was kept in the incubator overnight, allowing cells to attach on glass coverslips.

Cell washing, quenching, drying, and storage

A series of experiments with different procedures were performed to prepare cells, including washing, quenching, freeze drying, and storage, to evaluate their influences on cell metabolomics profiles (Figure 1).

Cell washing by cold ammonium formate (AF) solution. It has been reported AF solution (0.1427 M or 0.9%) is compatible with live cells and has a minimum influence on cell metabolism[5]. This washing step can replace nonvolatile salts (e.g., Na^+, K^+, and Mg^{2+} in culture medium) by volatile AF, significantly reducing matrix effect in SCMS experiment while minimizing alterations of metabolites in live cells. To perform cell washing, 0.9% of AF (w/w, 0.45 g in 50 mL LCMS-graded water (Fisher Chemical, USA)) were prepared and stored at 4°C. Next, 2 mL of cold AF solution was added into each empty well in a 12-well plate. Last, each coverslip containing cells was rapidly rinsed in a well containing AF solutions, and this washing step was repeated for the second time.

Cell quenching by LN_2. Rinsed cover slips containing cells were placed in an open Petri dish, which was placed into a container (e.g., folded by aluminum foil). 10−20 mL of LN_2 was carefully poured all over the Petri dish containing coverslips to ensure rapid freezing. Excessive LN_2 was cautiously removed by tilting the Petri dish with tweezer. This step must be carried out quickly to prevent formation of large ice crystals due to residual moisture from the earlier washing step.

Cell freeze drying in vacuum. Quenching was used to stop enzymatic activity at ultralow temperatures, whereas drying at low temperature removed water molecules from cells to deactivate enzymes during SCMS measurements under ambient conditions. Freeze drying was performed by placing cold Petri dish (with residual LN_2) containing coverslips into a SpeedVac (Thermo Scientific, Savant SPD111V). The rotor of the SpeedVac was removed to accommodate the Petri dish. Cell drying can be accomplished within 5−7 minutes following the standard drying procedures.

Cell storage in a -80 °C freezer. To test the influence of low temperature storage on cell's metabolomics profiles, dried cells were stored in a -80 °C freezer, aiming to minimize changes in cellular metabolites. After the storage for 48 h, dried cells were taken out from the -80 °C freezer and then immediately placed into a desiccator (at room temperature) to eliminate water condensation. Cells were maintained in the desiccator for ~10 min, allowing them to reach the room temperature prior to SCMS experiments.

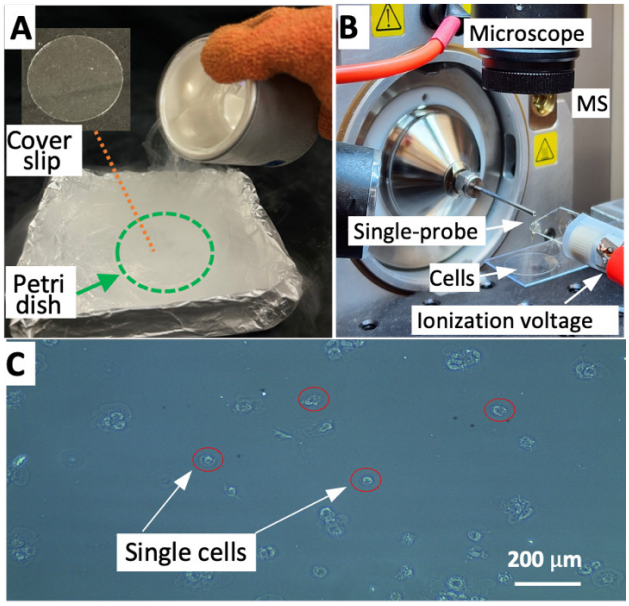

Figure 1. Cell quenching and SCMS setup. (A) Cell quenching by LN_2. The inset shows the cell containing glass cover slip in a Petri dish. (B) SCMS setup (C) Photo of cells after quenching.

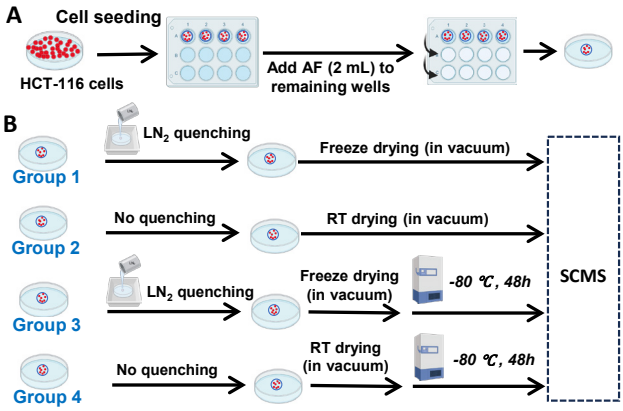

Figure 2. Overall workflow of SCMS studies of the impact of LN_2 quenching and -80 ℃ storage (48 h) on metabolites' profiles in single cells. (A) Cell seeding and washing by AF solution. (B) Four groups of cells were used in experiments. Group 1 – Cells were washed, quenched, and freeze dried (no storage); Group 2 – Cells were washed and dried at room temperature (RT)) (no quenching and storage); Group 3 – Cells were quenched, freeze dried, and stored; Group 4 – Cells were dried at RT and stored (no quenching).

To evaluate the influence of quenching and storage on cell metabolites, we prepared cells using different protocols and performed SCMS experiments (Figure 2). Four groups of cells (i.e., Groups 1, 2, 3, and 4) were prepared using different processes (Table 1, Figure 2B). Cells in all groups were washed by AF solution before undergoing additional processes.

Group 1. Cells in Group 1 underwent quenching and drying (no storage) prior to SCMS measurements. Cells in this group were served as the baseline control.

Group 2. To elucidate changes of cellular metabolites due to the omission of quenching, Group 2 represents freshly dried cells. Cells were dried in a vacuum at room temperature and subjected to SCMS analysis without low temperature storage.

Group 3. To determine if storage at low temperature can preserve cell metabolites, cells in Group 3 underwent quenching, drying, and storage (at -80 °C for 48h). This group of cells were prepared.

Group 4. To elucidate if storage at low temperature can preserve metabolites in freshly dried cells (no LN_2 quenching), cells in Group 4 underwent drying and storage (at -80 °C for 48h).

All four categories of cells were analyzed using the Single-probe SCMS method. 30 cells in each group were analyzed in both positive and negative ion modes, and 240 cells in total were measured. To minimize potential batch effects, glass coverslips containing cells from these four groups were placed on the XYZ-stage, and cells were randomly selected for measurements.

Table 1. Cell groups prepared using different processes for the Single-probe SCMS measurements. *

Cell groups	Cell preparation procedures		
	Quenching	Drying	Storage
1	Yes	Freeze	No
2	No	RT	No
3	Yes	Freeze	Yes (-80 °C, 48 h)
4	No	RT	Yes (-80 °C, 48 h)

*Cells were washed using AF solution (0.9%) prior to sequential processing. Washed cells were subjected to LN_2 quenching (Groups 2 and 4) or no quenching (Groups 1 and 3), dried (freeze drying or at room temperature (RT)) in a vacuum (SpeedVac) and analyzed without storage or after storage at -80 °C (48 h).

The Single-probe fabrication and SCMS setup

The Single-probe was fabricated in accordance with established procedures[35]. A Single-probe comprises three primary components: a nano-electrospray ionization (nano-ESI) emitter, a dual-bore quartz needle, and a fused silica capillary (Figure 3). The dual-bore quartz tubing (outer diameter 500 µm; inner diameter 127 µm, sourced from Friedrich & Dimmock, Millville, NJ) was pulled into sharp needles (tip size is ~10 µm) using a laser-based micropipette puller (Sutter P-2000, Sutter Instrument, Novato, CA). The nano-ESI emitter was pulled while heating a fused silica capillary (outer diameter 105 µm; inner diameter 40 µm; Polymicro Technologies, Phoenix, AZ) with a butane micro torch. The assembly of a Single-probe entails inserting the fused silica capillary and nano-ESI emitter into the dual-bore quartz needle. To facilitate experimentation, the Single-probe was affixed to a microscope glass slide using epoxy adhesive. Subsequently, the Single-probe was mounted on an XYZ-stage system, and digital microscope (Shenzhen D&F Co., China) was used to monitor cells during the experiment. The entire setup was coupled with an Orbitrap Exploris 240 mass spectrometer (Thermo Scientific, Waltham, MA, USA) for the analysis of SCMS (Figure S1). Acetonitrile (with 0.1% formic acid) served as the solvent for the SCMS experiments at a flowrate of 150 nL/min. The mass spectrometer was configured with mass ranges of m/z 200–1500 in positive ion mode and m/z 70-900 in negative ion mode. Additional mass spectrometer settings include a mass resolution of 120K (at m/z 200), ionization voltage of 2.9 kV in positive mode and −2.1 kV in negative ion mode, one microscan, a maximum injection time of 100 ms, and the use of an automatic gain control (AGC) Standard.

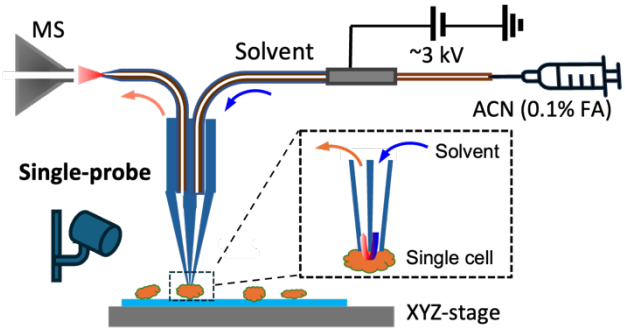

Figure 3. Single-probe SCMS setup for the analysis.

Data analysis

The raw SCMS data were subjected to pretreatment using a customized R script reported in our previous studies[45]. The data pretreatment includes background removal (to remove signals originating from solvents and cell culture media), noise reduction (to remove instrument noise), ion intensity normalization (to normalize the intensity of each ion to the total ion current (TIC)). Deisotope was performed with Python package ms_deisotope v0.0.053 (mobiusklein.github.io/ms_deisotope). After deisotope, peak alignment was performed using in-house Python script. To extract essential biological information and perform comparison of metabolomic profiles among different groups of cells, pretreated SCMS data were processed for visualization (by Principal Component Analysis (PCA), heat map, and volcano plot) and pathway analysis using MetaboAnalyst 6.0[74]. PCA was used for dimensionality reduction and visualization of SCMS data, allowing for intuitive comparison of the overall metabolites' profiles of cells from multiple groups. Heat map was generated to visualize the relative abundances of metabolites among cells. The volcano plot was used to illustrate significantly changed ($p < 0.05$ from t-test, $FC > 1.5$) species of cells in two different groups. Pathway analysis was employed to determine which metabolomic pathway significantly altered ($FDR < 0.05$) in pairwise comparison of cells in two groups. Pathway analysis examined the correlation between p-values (from pathway enrichment analysis) and pathway impact scores (from pathway topology analysis mapped against KEGG using Homo sapiens as the model organism). This comprehensive approach allowed for gaining deeper insights into the nuanced variations within the metabolic landscapes of the studied cell groups.

RESULT AND DISCUSSION

Due to rapid turnover rates of metabolites and relatively low throughput of most ambient SCMS techniques, cell metabolites may change during the extended measurement. To overcome these challenges, we developed a method, which integrates cell quenching, drying, and storage, to preserve cell metabolites for ambient SCMS metabolomics studies. Cells processed under

different conditions were analyzed using the Single-probe SCMS technique to evaluate the influence of experimental protocols on cell metabolites.

PCA illustrating the influence of sample preparation on overall metabolites' profiles in single cells

To visualize the overall profiles of metabolites in individual cells across four different groups, PCA was carried out to analyze the SCMS data collected in both positive (Figure 4A) and negative (Figure 4B) ion modes.

Positive ion mode results. A general trend can be observed: cells in Groups 1, 2, and 3 possess similar profiles of metabolites, whereas those in Group 4 largely distinguish them from the rest three groups. Two major conclusions can be drawn from these results. First, quenching and low temperature storage largely preserved metabolites in dried cells. As illustrated in Figure 4A, the overall metabolites' profiles between Group 1 (cells were freshly quenched and dried) and Group 3 (cells were quenched, dried, and stored at -80 °C for 48 h) are nearly indistinguishable. Storage at -80 °C is an effective way to preserve metabolites in quenched, dried cells. Second, freshly dried cells generally retained cell metabolites. The overall metabolomic profiles of cells in Group 1 and Group 2 (cells were dried without quenching) are largely indistinguishable. These results indicate that rapid vacuum drying at room temperature generally preserved cell metabolites when cells were analyzed soon (e.g., within 30 min) after drying. However, metabolites in unquenched cells changed after storage. Obvious difference of overall profiles of cell metabolites can be observed when comparing the results between Group 2 and Group 4 (unquenched cells, dried and stored at -80 °C). Similarly, significantly different metabolomics profiles can be observed between Group 3 and Group 4. Trends observed in PCA plots are also reflected from results obtained from Random Forest analysis (a higher classification error indicates a lower degree of distinguishment among groups). The classification error obtained from Group 4 (0.16) is lower than those from Groups 1 (0.27), 2 (0.44), and 3 (0.33), indicating that metabolites' profile in Group 4 is more different from the other three groups sharing more similarities (Table S1).

Negative ion mode results. Compared with results from the positive ion mode, metabolites' profiles of cells from Groups 1, 2, and 3 obtained in the negative ion mode seem to have lower degrees of overlap (Figures 4B), likely due to different detection sensitivities of molecules in the negative ion mode compared with the positive ion modes. However, the same trend was observed from Random Forest analysis: the classification error obtained from Group 4 (0.03) is lower than those from Groups 1 (0.25), 2 (0.29), and 3 (0.17) (Table S2). Thus, results from both ion modes indicate that quenching is indispensable to preserve cellular metabolomic integrity, even for cells to be stored under low a temperature such as -80 °C.

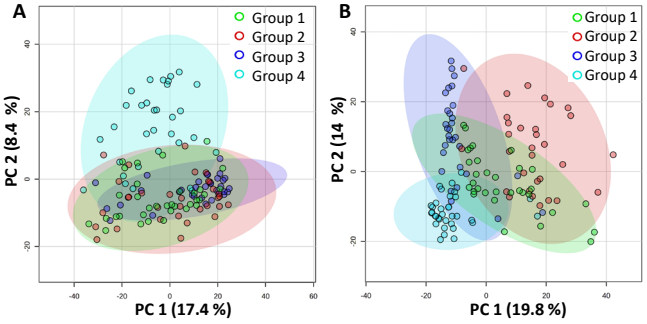

Figure 4. PCA of SCMS results obtained from cells in all four groups in the (A) positive and (B) negative ion modes.

Heat map illustrating the influence of sample preparation on metabolites' relative abundances in single cells

Heat maps were generated using SCMS data obtained from all four cell groups (Figure 5), depicting the changes in abundances of the top 100 metabolites in both positive (Figure 5A) and negative (Figure 5B) ionization modes. The rows represent different metabolites, and the columns represent individual cells, with colors indicating the relative abundance of each metabolite. Clear trends can be observed for metabolites across 120 single cells in four groups (with 30 single cells in each group).

Positive ion mode results. Notably, the heat map revealed patterns among cells in different groups. The positive ion mode results indicate that cells in Groups 1, 2, and 3 show similar patterns, with some minor transitions in Group 3, whereas those in Group 4 exhibit drastically different trends compared with the other three groups.

Negative ion mode results. Similar trends can be observed in the negative ion mode results, with more obvious transition can be observed in Group 3. Apparently, cells in Groups 1 and 2 show higher similarities in patterns of metabolomic abundances, indicating that quenching can largely preserve cell metabolites. In contrast, storing cells at low temperature without quenching had significantly altered metabolite profiles (Group 3 vs. Group 4). Although quenching can arrest cell metabolism, storage at as -80 °C for 48 h can still affect cell metabolites (Group 1 vs. Group 3).

Trends observed from heat maps are in good agreement with those obtained from PCA results. Our results indicate that the cells without quenching and after long-term storage (Group 4) had significantly altered metabolite profiles. Although storing quenched dried cells in at -80 °C seems to be a reasonable choice, the storage time should be reduced to minimize the alternations of cell metabolites.

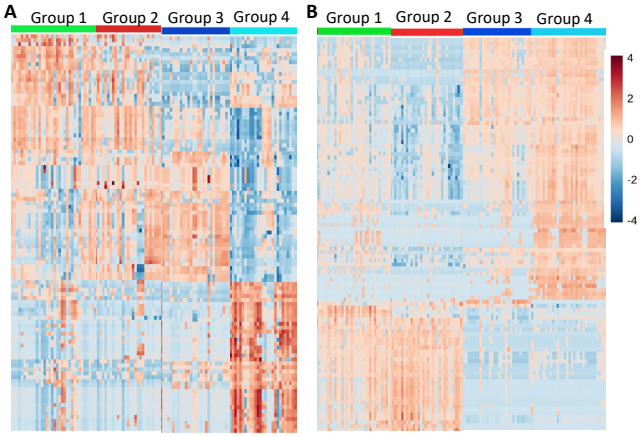

Figure 5. Heat maps summarizing metabolites measured in single HCT-116 cells under different preparation conditions. Relative abundances of top 100 metabolites in (A) positive and (B) negative ion modes.

Metabolites changed due to omitted quenching and during storage

Positive ion mode results. We investigated cell metabolites changed due to the omission of LN_2 quenching by comparing the SCMS data obtained from cells in Group 1 vs. Group 2 as well as Groups 3 vs. Group 4. For the comparison of Group 1 and Group 2, abundances of 60 metabolites were significantly changed with 22 increased and 38 decreased metabolites (Figure S2A) (p-value < 0.05, FC > 1.5)[75]. Pathway analysis did not identify any significantly impacted pathways (i.e., FDR > 0.05) (Table S3). For the comparison of Group 3 and Group 4, abundances of 378

metabolites were significantly altered (324 increased and 53 decreased) as illustrated in the volcano plot (Fig. S2B). We further conducted MS/MS analysis to identify those significantly altered ions at the single-cell level (Figure S3, Table S4). The decreased metabolites include phospholipids (e.g., phosphatidylcholines (PC (43:11), PC (41:11), PC (32:0), PC (35:8), and PC (30:0)), Lys phosphatidylcholine (LPC (34:0)), lysophosphatidic acid (LPA (24:5)), and glycerides (diglycerides (DG (30:2)). The increased metabolites include phospholipids (PC (40:7), PC (36:2), PC (34:2), PC (37:7), PC (35:6), sphingomyelins (SM (45:1)), and cholesteryl esters CE (18:3). Results from pathway analysis of significantly altered species, including both identified and tentatively labeled metabolites, resulted in multiple significantly changed pathways (Figure S4, Table S5), including galactose metabolism, starch and sucrose metabolism, arachidonic acid metabolism, linoleic acid metabolism, biosynthesis of unsaturated fatty acids, and steroid biosynthesis pathway.

To evaluate the impact of the storage at -80 °C on cell metabolites, we performed comparisons between Group 1 and Group 3 as well as between Group 2 and Group 4. We discovered increased (58) and decreased (134) metabolites in the comparison of Group 1 vs. Group 3 (Figure S2C). Pathway analysis based on tentatively labeled metabolites did not reveal any pathway significantly impacted (Table S6). The comparison between Group 2 and Group 4 showed 144 increased and 100 decreased metabolites (Figure S2D). Pathway analysis based on tentatively labeled metabolites revealed that galactose metabolism and starch and sucrose metabolism were significantly impacted (Figure S5, Table S7).

Negative ion mode results. In alignment with the positive mode analysis, we performed similar comparisons using the negative ion mode data. To investigate cell metabolites changed due to the omission of LN_2 quenching, we investigated the SCMS data obtained from cells in Group 1 vs. Group 2 as well as Groups 3 vs. Group 4. For comparison between Group 1 and Group 2, 145 metabolites were significantly changed with 20 increased and 125 decreased metabolites (Figure S6A). Pathway analysis revealed that galactose metabolism (Figure S7) significantly changed (Table S8). For comparison between Group 3 and Group 4, our results show that the abundances of 291 metabolites were significantly altered (Figure S6B), with 235 increased and 56 decreased metabolites. Using MS/MS analysis at the single-cell level, we identified multiple metabolites, including increased oleic acid and fatty acid FA (17:3) as well as deceased triglycerides TG (51:14) (Figure S8) (Table S4). Tentatively labeled species include decreased lipids (e.g., phosphatidylglycerols (PG(33:4), PG(43:4), PG(33:5), PG(32:4)), DG (38:5), DG (35:4), and sphingomyelins (SM(36:5), SM(36:6)) and increased organic acids (linoleic acid, succinic acid, and octadecenoic acid), lipid (MG (22:4)), and other small molecules (alpha-D-glucose and creatine). Significantly altered metabolites in the comparison of Groups 3 and Group 4 indicate substantially affected pathways, suggesting that storing samples at -80 °C without quenching is insufficient to preserve metabolomic integrity. Analysis of tentatively labeled metabolites revealed that 11 metabolic pathways were significantly affected due to storage without quenching (Table S9). These pathways include alanine, aspartate, and glutamate metabolism, D-amino acid metabolism, butanoate metabolism, linoleic acid metabolism, galactose metabolism, arginine and proline metabolism, valine, leucine, and isoleucine biosynthesis, valine, leucine, and isoleucine degradation, glycine, serine, and threonine metabolism, pantothenate and CoA biosynthesis, and caffeine (Figure S9).

To investigate the influence of low temperature storage on cell metabolites' profiles, we performed the same comparison (Group 1 vs. Group 3 and Group 2 vs. Group 4). The comparison between Group 1 and Group 3 revealed 86 increased and 141 decreased metabolites (Figure S6C). Pathway analysis demonstrated that multiple pathways were significantly affected (Figure S10, Table S10): arachidonic acid metabolism, arginine and proline metabolism, linoleic acid metabolism, D-Amino acid metabolism, valine, leucine and isoleucine biosynthesis, pantothenate and CoA biosynthesis, alanine, aspartate and glutamate metabolism, and Galactose metabolism. In the comparison between Group 2 and Group 4, 87 metabolites were increased and 187 were decreased (Figure S5D). Three metabolic pathways were significantly impacted (Figure S11, Table S11): arachidonic acid metabolism, valine, leucine and isoleucine biosynthesis, and galactose metabolism.

Our results obtained from both positive and negative ion modes indicate LN_2 quenching is indispensable to preserve metabolites, but storage at low temperature (even at -80 °C) should be minimized to retain cell metabolites. Although rapid drying in vacuum at room temperature can largely retain cell metabolites, cells need to be immediately analyzed after drying because storage at -80 °C can still change cell metabolites. Compared with freeze drying, which forms small ice crystals with porous structures and large surface areas, drying at room temperatures is less effective to remove water molecules from cells[76]. It is possible that residual water content in cells as well as the condensed water, which could be possibly formed during the defrosting process (e.g., during the transition from the -80°C freezer to the desiccator and due to residual moisture in the desiccator), could result in partial rehydration of dried cells lead to reactions such as through reactivated enzymatic activities and hydrolysis reactions.

CONCLUSION

In this study, live HCT-116 cells were washed by ammonium formate solution, quenched by LN_2, freeze-dried in a vacuum, and stored in a -80 ℃ freezer. We then performed single-cell metabolomics studies using the Single-probe SCMS technique. Our results indicated that washing using ammonium formate led to enhancement in ion intensities attributed to the mitigated matrix effect. Remarkably, a diverse array of lipids, including PC, PS, PE, PA, PG, TG, DG, and MG were identified from individual cells. We further studied the influence of LN_2 quenching and storage at -80 °C on metabolites and metabolomic pathways. Notably, LN_2 quenching and freeze-drying preserved cells' metabolomic profiles. Storage of LN_2 quenched cells at -80 ℃ for 48 h generally retained cell metabolites, enabling reliable SCMS experiments with extended time or low temperature shipped samples. However, the time delay between LN_2 quenching and SCMS experiments should be minimized. Although cells underwent rapid drying in vacuum at room temperature could largely retain metabolites, cells need to be immediately analyzed because storage (even at -80 ℃ for 48 h) could change metabolites' compositions. These findings collectively contribute to the sample preparation techniques in single-cell metabolomics studies. The developed methods can be readily adopted by researchers using other ambient-based SCMS techniques for broad applications.

ASSOCIATED CONTENT

Supporting Information

The Supporting Information is available free of charge on the ACS Publications website.

Results of random forest analysis of SCMS; pathway analysis; volcano plots illustrating significantly changed species; significant peaks identified using MS/MS identification in single cells; experimental SCMS setup of the Single-probe coupled to Thermo Orbitrap Exploris 240 mass spectrometer.

AUTHOR INFORMATION

Corresponding Author

* Zhibo Yang - [1]Department of Chemistry and Biochemistry, University of Oklahoma, Norman, Oklahoma 73019, United States;
[2]Stephenson Cancer Center, University of Oklahoma Health Sciences Center, Oklahoma City, OK, 73104, United States
Email: Zhibo.Yang@ou.edu

Author

Shakya Wije Munige‡ - Department of Chemistry and Biochemistry, University of Oklahoma, Norman, Oklahoma, US, 73019; Email: shakya.sankalpani.gunasena.wije.munige-1@ou.edu
Deepti Bhusal‡ - Department of Chemistry and Biochemistry, University of Oklahoma, Norman, Oklahoma, US, 73019; Email: deepti.bhusal-1@ou.edu
Zongkai Peng - Department of Chemistry and Biochemistry, University of Oklahoma, Norman, Oklahoma, US, 73019; Email: Zongkai.Peng-1@ou.edu
Dan Chen – Department of Chemistry and Biochemistry, University of Oklahoma, Norman, Oklahoma, US, 73019; Email: Dan.Chen@ou.edu

Author Contributions

‡S.W.M. and D.B. contributed equally to this paper.

Notes
The authors declare no competing financial interest.

Data Availability
Raw data from SCMS experiments can be accessed in the MASSIVE database under the accession MSV000096378. Python code for SCMS data alignment is available on GitHub https://github.com/dandandan001/SCMS-data-alignment

ACKNOWLEDGMENT

We greatly appreciate the support from the National Science Foundation (2305182), National Institutes of Health (1R01AI177469), and Chan Zuckerberg Initiative.

REFERENCES

(1) Lee, S.; Vu, H. M.; Lee, J. H.; Lim, H.; Kim, M. S. Advances in Mass Spectrometry-Based Single Cell Analysis. *Biology (Basel)* **2023**, *12* (3). DOI: 10.3390/biology12030395.
(2) Rubakhin, S. S.; Romanova, E. V.; Nemes, P.; Sweedler, J. V. Profiling metabolites and peptides in single cells. *Nat Methods* **2011**, *8* (4 Suppl), S20-29. DOI: 10.1038/nmeth.1549.
(3) Alberts, D. B., J Lewis, M Raft, K Roberts and J D Watson. ISBN 0-8153-1619-4. *Molecular biology of cell*; Garland Publishing, 1994.
(4) Luby-Phelps, K. Cytoarchitecture and physical properties of cytoplasm: volume, viscosity, diffusion, intracellular surface area. *Int Rev Cytol* **2000**, *192*, 189-221. DOI: 10.1016/s0074-7696(08)60527-6.
(5) Zhang, X. C.; Zang, Q.; Zhao, H.; Ma, X.; Pan, X.; Feng, J.; Zhang, S.; Zhang, R.; Abliz, Z.; Zhang, X. Combination of Droplet Extraction and Pico-ESI-MS Allows the Identification of Metabolites from Single Cancer Cells. *Anal Chem* **2018**, *90* (16), 9897-9903. DOI: 10.1021/acs.analchem.8b02098.
(6) Milo, R. What is the total number of protein molecules per cell volume? A call to rethink some published values. *Bioessays* **2013**, *35* (12), 1050-1055. DOI: 10.1002/bies.201300066.
(7) Matthias Heinemann, R. Z. Metabolomics: small molecules, single cells. *Nature* **2016**, *540*, 3.
(8) Gawad, C.; Koh, W.; Quake, S. R. Single-cell genome sequencing: current state of the science. *Nat Rev Genet* **2016**, *17* (3), 175-188. DOI: 10.1038/nrg.2015.16.
(9) Schwartzman, O.; Tanay, A. Single-cell epigenomics: techniques and emerging applications. *Nat Rev Genet* **2015**, *16* (12), 716-726. DOI: 10.1038/nrg3980.
(10) Kanter, I.; Kalisky, T. Single cell transcriptomics: methods and applications. *Front Oncol* **2015**, *5*, 53. DOI: 10.3389/fonc.2015.00053.
(11) Newman, J. R.; Ghaemmaghami, S.; Ihmels, J.; Breslow, D. K.; Noble, M.; DeRisi, J. L.; Weissman, J. S. Single-cell proteomic analysis of S. cerevisiae reveals the architecture of biological noise. *Nature* **2006**, *441* (7095), 840-846. DOI: 10.1038/nature04785.
(12) Rubakhin, S. S.; Lanni, E. J.; Sweedler, J. V. Progress toward single cell metabolomics. *Current opinion in biotechnology* **2013**, *24* (1), 95-104, DOI: 10.1016/j.copbio.2012.10.021.
(13) Johnson, C. H.; Gonzalez, F. J. Challenges and opportunities of metabolomics. *J Cell Physiol* **2012**, *227* (8), 2975-2981. DOI: 10.1002/jcp.24002.
(14) Kellyn B; Keegan Sawyer, R. In *Use of Metabolomics to Advance Research on Environmental Exposures and the Human Exposome: Workshop in Brief*, The National Academies Collection: Reports funded by National Institutes of Health, 2016.
(15) Yang, Y.; Huang, Y.; Wu, J.; Liu, N.; Deng, J.; Luan, T. Single-cell analysis by ambient mass spectrometry. *TrAC Trends in Analytical Chemistry* **2017**, *90*, 14-26. DOI: 10.1016/j.trac.2017.02.009.
(16) Chen, X.; Peng, Z.; Yang, Z. Metabolomics studies of cell-cell interactions using single cell mass spectrometry combined with fluorescence microscopy. *Chem Sci* **2022**, *13* (22), 6687-6695. DOI: 10.1039/d2sc02298b.
(17) Hong, S.; Pawel, G. T.; Pei, R.; Lu, Y. Recent progress in developing fluorescent probes for imaging cell metabolites. *Biomed Mater* **2021**, *16* (4). DOI: 10.1088/1748-605X/abfd11.
(18) Zhang, X. C.; Wei, Z. W.; Gong, X. Y.; Si, X. Y.; Zhao, Y. Y.; Yang, C. D.; Zhang, S. C.; Zhang, X. R. Integrated Droplet-Based Microextraction with ESI-MS for Removal of Matrix Interference in Single-Cell Analysis. *Sci Rep* **2016**, *6*, 24730. DOI: 10.1038/srep24730.
(19) Zhang, L.; Vertes, A. Single-Cell Mass Spectrometry Approaches to Explore Cellular Heterogeneity. *Angew Chem Int Ed Engl* **2018**, *57* (17), 4466-4477. DOI: 10.1002/anie.201709719.
(20) Duncan, K. D.; Fyrestam, J.; Lanekoff, I. Advances in mass spectrometry based single-cell metabolomics. *Analyst* **2019**, *144* (3), 782-793. DOI: 10.1039/c8an01581c.
(21) Lan, Y.; Zou, Z.; Yang, Z. Single Cell mass spectrometry: Towards quantification of small molecules in individual cells. *TrAC Trends in Analytical Chemistry* **2024**, *174*, 117657. DOI: https://doi.org/10.1016/j.trac.2024.117657.
(22) Liu, R. M.; Yang, Z. B. Single cell metabolomics using mass spectrometry: Techniques and data analysis. *Anal Chim Acta* **2021**, *1143*, 124-134. DOI: 10.1016/j.aca.2020.11.020.
(23) Ibanez, A. J.; Fagerer, S. R.; Schmidt, A. M.; Urban, P. L.; Jefimovs, K.; Geiger, P.; Dechant, R.; Heinemann, M.; Zenobi, R. Mass spectrometry-based metabolomics of single yeast cells. *Proc Natl Acad Sci U S A* **2013**, *110* (22), 8790-8794. DOI: 10.1073/pnas.1209302110.
(24) Monge, M. E.; Harris, G. A.; Dwivedi, P.; Fernandez, F. M. Mass spectrometry: recent advances in direct open air surface sampling/ionization. *Chem Rev* **2013**, *113* (4), 2269-2308. DOI: 10.1021/cr300309q.
(25) Huang, M. Z.; Yuan, C. H.; Cheng, S. C.; Cho, Y. T.; Shiea, J. Ambient ionization mass spectrometry. *Annu Rev Anal Chem (Palo Alto Calif)* **2010**, *3*, 43-65. DOI: 10.1146/annurev.anchem.111808.073702.
(26) Vertes, B. S. A. In Situ Metabolic Profiling of Single Cells by Laser Ablation Electrospray Ionization Mass Spectrometry. *Anal. Chem.* **2009**, *81*, 6.
(27) Naohiro Tsuyama, H. M., Emi Tokunaga, and Tsutomu Masujima. Live Single-Cell Molecular Analysis by Video-Mass Spectrometry. *Analytical Sciences* **2008**, *24*, 3.
(28) Bergman, H. M.; Lanekoff, I. Profiling and quantifying endogenous molecules in single cells using nano-DESI MS. *Analyst* **2017**, *142* (19), 3639-3647. DOI: 10.1039/c7an00885f.
(29) Gong, X.; Zhao, Y.; Cai, S.; Fu, S.; Yang, C.; Zhang, S.; Zhang, X. Single cell analysis with probe ESI-mass spectrometry: detection of metabolites at cellular and subcellular levels. *Anal Chem* **2014**, *86* (8), 3809-3816. DOI: 10.1021/ac500882e.
(30) Chen, F.; Lin, L.; Zhang, J.; He, Z.; Uchiyama, K.; Lin, J. M. Single-Cell Analysis Using Drop-on-Demand Inkjet Printing and Probe Electrospray Ionization Mass Spectrometry. *Anal Chem* **2016**, *88* (8), 4354-4360. DOI: 10.1021/acs.analchem.5b04749.
(31) Huang, Q.; Mao, S.; Khan, M.; Li, W.; Zhang, Q.; Lin, J. M. Single-cell identification by microfluidic-based in situ extracting and online mass spectrometric analysis of phospholipids expression. *Chem Sci* **2019**, *11* (1), 253-256. DOI: 10.1039/c9sc05143k.

(32) Xu, S.; Liu, M.; Bai, Y.; Liu, H. Multi-Dimensional Organic Mass Cytometry: Simultaneous Analysis of Proteins and Metabolites on Single Cells. *Angew Chem Int Ed Engl* **2021**, *60* (4), 1806-1812. DOI: 10.1002/anie.202009682.
(33) Huang, Q.; Mao, S.; Khan, M.; Lin, J. M. Single-cell assay on microfluidic devices. *Analyst* **2019**, *144* (3), 808-823. DOI: 10.1039/c8an01079j.
(34) Spitzer, M. H.; Nolan, G. P. Mass Cytometry: Single Cells, Many Features. *Cell* **2016**, *165* (4), 780-791. DOI: 10.1016/j.cell.2016.04.019 .
(35) Pan, N.; Rao, W.; Kothapalli, N. R.; Liu, R.; Burgett, A. W.; Yang, Z. The single-probe: a miniaturized multifunctional device for single cell mass spectrometry analysis. *Anal Chem* **2014**, *86* (19), 9376-9380. DOI: 10.1021/ac5029038.
(36) Liu, R.; Zhang, G.; Yang, Z. Towards rapid prediction of drug-resistant cancer cell phenotypes: single cell mass spectrometry combined with machine learning. *Chem Commun (Camb)* **2019**, *55* (5), 616-619. DOI: 10.1039/c8cc08296k.
(37) Rao, W.; Pan, N.; Yang, Z. Applications of the Single-probe: Mass Spectrometry Imaging and Single Cell Analysis under Ambient Conditions. *J Vis Exp* **2016**, (112). DOI: 10.3791/53911.
(38) Sun, M.; Tian, X.; Yang, Z. Microscale Mass Spectrometry Analysis of Extracellular Metabolites in Live Multicellular Tumor Spheroids. *Anal Chem* **2017**, *89* (17), 9069-9076. DOI: 10.1021/acs.analchem.7b01746.
(39) Liu, R.; Pan, N.; Zhu, Y.; Yang, Z. T-Probe: An Integrated Microscale Device for Online In Situ Single Cell Analysis and Metabolic Profiling Using Mass Spectrometry. *Anal Chem* **2018**, *90* (18), 11078-11085. DOI: 10.1021/acs.analchem.8b02927.
(40) Zhu, Y.; Liu, R.; Yang, Z. Redesigning the T-probe for mass spectrometry analysis of online lysis of non-adherent single cells. *Anal Chim Acta* **2019**, *1084*, 53-59. DOI: 10.1016/j.aca.2019.07.059.
(41) Zhu, Y.; Wang, W.; Yang, Z. Combining Mass Spectrometry with Paterno-Buchi Reaction to Determine Double-Bond Positions in Lipids at the Single-Cell Level. *Anal Chem* **2020**, *92* (16), 11380-11387. DOI: 10.1021/acs.analchem.0c02245.
(42) Liu, R.; Li, J.; Lan, Y.; Nguyen, T. D.; Chen, Y. A.; Yang, Z. Quantifying Cell Heterogeneity and Subpopulations Using Single Cell Metabolomics. *Anal Chem* **2023**, *95* (18), 7127-7133. DOI: 10.1021/acs.analchem.2c05245.
(43) Pan, N.; Rao, W.; Standke, S. J.; Yang, Z. Using Dicationic Ion-Pairing Compounds To Enhance the Single Cell Mass Spectrometry Analysis Using the Single-Probe: A Microscale Sampling and Ionization Device. *Anal Chem* **2016**, *88* (13), 6812-6819. DOI: 10.1021/acs.analchem.6b01284.
(44) Standke, S. J.; Colby, D. H.; Bensen, R. C.; Burgett, A. W. G.; Yang, Z. Mass Spectrometry Measurement of Single Suspended Cells Using a Combined Cell Manipulation System and a Single-Probe Device. *Anal Chem* **2019**, *91* (3), 1738-1742. DOI: 10.1021/acs.analchem.8b05774.
(45) Liu, R.; Zhang, G.; Sun, M.; Pan, X.; Yang, Z. Integrating a generalized data analysis workflow with the Single-probe mass spectrometry experiment for single cell metabolomics. *Anal Chim Acta* **2019**, *1064*, 71-79. DOI: 10.1016/j.aca.2019.03.006.
(46) Nguyen, T. D.; Lan, Y.; Kane, S. S.; Haffner, J. J.; Liu, R.; McCall, L. I.; Yang, Z. Single-Cell Mass Spectrometry Enables Insight into Heterogeneity in Infectious Disease. *Anal Chem* **2022**, *94* (30), 10567-10572. DOI: 10.1021/acs.analchem.2c02279.
(47) Pan, N.; Standke, S. J.; Kothapalli, N. R.; Sun, M.; Bensen, R. C.; Burgett, A. W. G.; Yang, Z. Quantification of Drug Molecules in Live Single Cells Using the Single-Probe Mass Spectrometry Technique. *Anal Chem* **2019**, *91* (14), 9018-9024. DOI: 10.1021/acs.analchem.9b01311.
(48) Sun, M.; Yang, Z. Metabolomic Studies of Live Single Cancer Stem Cells Using Mass Spectrometry. *Anal Chem* **2019**, *91* (3), 2384-2391. DOI: 10.1021/acs.analchem.8b05166.
(49) Lan, Y.; Chen, X.; Yang, Z. Quantification of Nitric Oxide in Single Cells Using the Single-Probe Mass Spectrometry Technique. *Anal Chem* **2023**, *95* (51), 18871-18879. DOI: 10.1021/acs.analchem.3c04393.
(50) Chen, X.; Sun, M.; Yang, Z. Single cell mass spectrometry analysis of drug-resistant cancer cells: Metabolomics studies of synergetic effect of combinational treatment. *Anal Chim Acta* **2022**, *1201*, 339621. DOI: 10.1016/j.aca.2022.339621.
(51) Chen, X; Sun, M.; Yang, Z. Single Cell Mass Spectrometry Analysis of Drug-Resistant Cancer Cells- Metabolomics Studies of Synergetic Effect of Combinational Treatment. *Anal Chim Acta* **2022**, 1201, 339621. DOI: 10.1016/j.aca.2022.339621.
(52) Sun, M.; Chen, X.; Yang, Z. Single cell mass spectrometry studies reveal metabolomic features and potential mechanisms of drug-resistant cancer cell lines. *Anal Chim Acta* **2022**, *1206*, 339761. DOI: 10.1016/j.aca.2022.339761.
(53) Portero, E. P.; Nemes, P. Dual cationic-anionic profiling of metabolites in a single identified cell in a live Xenopus laevis embryo by microprobe CE-ESI-MS. *Analyst* **2019**, *144* (3), 892-900. DOI: 10.1039/c8an01999a.
(54) Guo, S.; Zhang, C.; Le, A. The limitless applications of single-cell metabolomics. *Current Opinion in Biotechnology* **2021**, *71*, 115-122.
(55) Buziol, S.; Bashir, I.; Baumeister, A.; Claassen, W.; Noisommit-Rizzi, N.; Mailinger, W.; Reuss, M. New bioreactor-coupled rapid stopped-flow sampling technique for measurements of metabolite dynamics on a subsecond time scale. *Biotechnol Bioeng* **2002**, *80* (6), 632-636. DOI: 10.1002/bit.10427.
(56) Sake, C. L.; Newman, D. M.; Boyle, N. R. Evaluation of quenching methods for metabolite recovery in photoautotrophic Synechococcus sp. PCC 7002. *Biotechnol Prog* **2020**, *36* (5), e3015. DOI: 10.1002/btpr.3015.
(57) Wang, T.; Wang, X.; Zhuang, Y.; Wang, G. A systematic evaluation of quenching and extraction procedures for quantitative metabolome profiling of HeLa carcinoma cell under 2D and 3D cell culture conditions. *Biotechnol J.* **2023**, *18* (5).
(58) Hernandez Bort, J. A.; Shanmukam, V.; Pabst, M.; Windwarder, M.; Neumann, L.; Alchalabi, A.; Krebiehl, G.; Koellensperger, G.; Hann, S.; Sonntag, D.; et al. Reduced quenching and extraction time for mammalian cells using filtration and syringe extraction. *J Biotechnol* **2014**, *182-183* (100), 97-103. DOI: 10.1016/j.jbiotec.2014.04.014.
(59) House, R. R. J.; Soper-Hopper, M. T.; Vincent, M. P.; Ellis, A. E.; Capan, C. D.; Madaj, Z. B.; Wolfrum, E.; Isaguirre, C. N.; Castello, C. D.; Johnson, A. B.; et al. A diverse proteome is present and enzymatically active in metabolite extracts. *Nat Commun* **2024**, *15* (1), 5796. DOI: 10.1038/s41467-024-50128-z.
(60) Andrea Amantonico, P. L. U., Stephan R. Fagerer, Roman M. Balabin, and Renato Zenobi. Single-Cell MALDI-MS as an Analytical Tool for Studying Intrapopulation Metabolic Heterogeneity of Unicellular Organisms.pdf. *Anal. Chem.* **2010**, *82*, 6. DOI: 10.1007/s00216-00010-03850-00211.
(61) Sellick, C. A.; Hansen, R.; Maqsood, A. R.; Dunn, W. B.; Stephens, G. M.; Goodacre, R.; Dickson, A. J. Effective Quenching Processes for Physiologically Valid Metabolite Profiling of Suspension Cultured Mammalian Cells. *Analytical Chemistry* **December 5, 2008**, *81* (1). DOI: 10.1021/ac8016899.
(62) Volmer, M.; Northoff, S.; Scholz, S.; Thute, T.; Buntemeyer, H.; Noll, T. Fast filtration for metabolome sampling of suspended animal cells. *Biotechnol Lett* **2011**, *33* (3), 495-502. DOI: 10.1007/s10529-010-0466-7.
(63) Dietmair, S.; Timmins, N. E.; Gray, P. P.; Nielsen, L. K.; Kromer, J. O. Towards quantitative metabolomics of mammalian cells: development of a metabolite extraction protocol. *Anal Biochem* **2010**, *404* (2), 155-164. DOI: 10.1016/j.ab.2010.04.031.
(64) Faijes, M.; Mars, A. E.; Smid, E. J. Comparison of quenching and extraction methodologies for metabolome analysis of Lactobacillus plantarum. *Microb Cell Fact* **2007**, *6*, 27. DOI: 10.1186/1475-2859-6-27.
(65) Pabst, M.; Grass, J.; Fischl, R.; Léonard, R.; Jin, C.; Hinterkörner, G.; Borth, N.; Altmann, F. Nucleotide and Nucleotide Sugar Analysis by Liquid Chromatography-Electrospray Ionization-Mass Spectrometry on Surface-Conditioned Porous Graphitic Carbon. *Anal. Chem.* **2010**, *82* (23), 9782-8. DOI: 10.1021/ac101975k.
(66) Lorenz, M. A.; Burant, C. F.; Kennedy, R. T. Reducing time and increasing sensitivity in sample preparation for adherent mammalian cell metabolomics. *Anal Chem* **2011**, *83* (9), 3406-3414. DOI: 10.1021/ac103313x.
(67) Wahrheit, J.; Heinzle, E. Quenching methods for the analysis of intracellular metabolites. *Methods Mol Biol* **2014**, *1104*, 211-221. DOI: 10.1007/978-1-62703-733-4_14.
(68) Volmer, M.; Gettmann, J.; Scholz, S.; Buntemeyer, H.; Noll, T. A method for metabolomic sampling of suspended animal cells using fast filtration. *BMC Proc* **2011**, *5 Suppl 8* (Suppl 8), P93. DOI: 10.1186/1753-6561-5-S8-P93.
(69) Richard King, R. B., Carmen Fernandez-Metzler,; Cynthia Miller-Stein, a. T. O. Mechanistic Investigation of Ionization Suppression in Electrospray Ionization. *J Am Soc Mass Spectrom* **2000**, *11*, 8.
(70) Dunn, W. B. Current trends and future requirements for the mass spectrometric investigation of microbial, mammalian and plant metabolomes. *Phys Biol* **2008**, *5* (1), 011001. DOI: 10.1088/1478-3975/5/1/011001.
(71) Pinu, F. R.; Villas-Boas, S. G.; Aggio, R. Analysis of Intracellular Metabolites from Microorganisms: Quenching and Extraction Protocols. *Metabolites* **2017**, *7* (4). DOI: 10.3390/metabo7040053.

(72) Krismer, J.; Sobek, J.; Steinhoff, R. F.; Fagerer, S. R.; Pabst, M.; Zenobi, R. Screening of Chlamydomonas reinhardtii Populations with Single-Cell Resolution by Using a High-Throughput Microscale Sample Preparation for Matrix-Assisted Laser Desorption Ionization Mass Spectrometry. *Appl Environ Microbiol* **2015**, *81* (16), 5546-5551. DOI: 10.1128/AEM.01201-15.
(73) Ye, D.; Li, X.; Wang, C.; Liu, S.; Zhao, L.; Du, J.; Xu, J.; Li, J.; Tian, L.; Xia, X. Improved Sample Preparation for Untargeted Metabolomics Profiling of Escherichia coli. *Microbiol Spectr* **2021**, *9* (2), e0062521. DOI: 10.1128/Spectrum.00625-21.
(74) Pang, Z.; Lu, Y.; Zhou, G.; Hui, F.; Xu, L.; Viau, C.; Spigelman, A. F.; MacDonald, P. E.; Wishart, D. S.; Li, S.; et al. MetaboAnalyst 6.0: towards a unified platform for metabolomics data processing, analysis and interpretation. *Nucleic Acids Res* **2024**, *52* (W1), W398-W406. DOI: 10.1093/nar/gkae253.
(75) Renmeng Liu, Z. Y. Single cell metabolomics using mass spectrometry- Techniques and data analysis. *Analytica Chimica Acta* **2021**, *1143*, 11.
(76) Rockinger, U.; Funk, M.; Winter, G. Current Approaches of Preservation of Cells During (freeze-) Drying. *J Pharm Sci* **2021**, *110* (8), 2873-2893. DOI: 10.1016/j.xphs.2021.04.018.

Developing Cell Quenching Method to Facilitate Single Cell Mass Spectrometry Metabolomics Studies

Shakya Wije Munige[#a], Deepti Bhusal[#a], Zongkai Peng[a], Dan Chen[a], Zhibo Yang[*a,b]

[a] Department of Chemistry and Biochemistry, University of Oklahoma, Norman, Oklahoma, 73019, US

[b] Stephenson Cancer Center, University of Oklahoma Health Sciences Center, Oklahoma City, Oklahoma, 73104, US

[#]These authors contributed equally

[*] Corresponding author

Email: Zhibo.Yang@ou.edu

Table of Contents

Supporting Tables

Table S1. Random forest analysis of SCMS results obtained from the positive ion mode.

	Group 1	Group 2	Group 3	Group 4	Classification Error
Group 1	25	3	4	2	0.27
Group 2	7	18	5	2	0.44
Group 3	7	3	22	2	0.33
Group 4	1	1	3	27	0.16

Table S2. Random forest analysis of SCMS results obtained from the negative ion mode.

	Group 1	Group 2	Group 3	Group 4	Classification Error
Group 1	24	7	1	0	0.25
Group 2	7	22	2	0	0.29
Group 3	1	1	25	3	0.17
Group 4	1	0	0	33	0.03

Table S3. Pathway analysis of Group 1 vs. Group 2 SCMS results in the positive ion mode. *

Pathways	Total	Expected	Hits	Raw p	-log10(p)	Holm adjust	FDR	Impact
Steroid hormone biosynthesis	87	0.55238	4	0.0014136	2.8497	0.11309	0.11309	0.06273
Ubiquinone and other terpenoid-quinone biosynthesis	18	0.11429	2	0.0052607	2.279	0.41559	0.21043	0.38462
Sphingolipid metabolism	32	0.20317	2	0.016262	1.7888	1	0.43364	0.35835
Linoleic acid metabolism	5	0.031746	1	0.031385	1.5033	1	0.6277	0
Glycerophospholipid metabolism	36	0.22857	1	0.20697	0.68409	1	1	0.01896

*No metabolomic pathway was affected significantly (FDR < 0.05) by rapid drying at room temperature (RT) without storage. Cells were washed by ammonium formate and dried in a vacuum.

Table S4. MS/MS identified metabolites significantly changed in positive mode. *

m/z	Molecular Formula	Adduct	Compound	NCE HCD
882.5668**	C51H80NO9P	[M+H]+	PC (43:11)	10
879.7378	C50H101N2O6P	[M+Na]+	SM(45:1)	30
856.5645	C48H84NO7P	[M+K]+	PC (40:7)	10
854.5352**	C49H76NO9P	[M+H]+	PC(41:11)	10
812.5152	C45H76NO8P	[M+Na]+	PC(37:7)	25
808.5793	C44H84NO8P	[M+Na]+	PC(36:2)	20
772.6113**	C42H88NO7P	[M+Na]+	LPC (34:0)	25
772.5226	C43H76NO7P	[M+Na]+	PC(35:6)	20
768.491**	C43H72NO7P	[M+Na]+	PC (35:8)	20
744.5875	C42H82NO7P	[M+H]+	PC (34:2)	18
734.5674**	C40H80NO8P	[M+H]+	PC(32:0)	20
706.5353	C38H76NO8P	[M+H]+	PC(30:0)	20
685.5505	C45H74O3	[M+Na]+	CE (18:3);O	20
537.2759**	C27H47O6P	[M+K]+	LPA O-24:5	25
523.4705	C33H62O4	[M+Na]+	DG (30:2)	15
281.2482	C18H34O2	[M-H]-	FA (18:1) Oleic acid	35
327.18	C17H28O6	[M-H]-	FA (17:3);O4	20
425.2712**	C54H76O8	[M-2H]2-	TG(51:14)	25

*Features in Figures S2 and S7 were identified using MS/MS analysis of positive (red font) and negative (black font) ions at the single-cell level.
**Upregulated metabolites.

Table S5. Pathway analysis of Group 3 vs. Group 4 SCMS results in the positive ion mode. *

Pathways	Total	Expected	Hits	Raw p	-log10(p)	Holm adjust	FDR	Impact
Galactose metabolism	27	1.3371	11	1.4907E-08	7.8266	1.1925E-06	1.1925E-06	0.70254
Starch and sucrose metabolism	18	0.89143	7	1.1453E-05	4.9411	0.00090478	0.00045812	0.54856
Arachidonic acid metabolism	44	2.179	8	0.0010475	2.9798	0.081705	0.021767	0.37522
Linoleic acid metabolism	5	0.24762	3	0.0010883	2.9632	0.083803	0.021767	1
Biosynthesis of unsaturated fatty acids	36	1.7829	7	0.0014544	2.8373	0.11053	0.02327	0
Steroid biosynthesis	41	2.0305	7	0.003204	2.4943	0.2403	0.04272	0.16089
Drug metabolism - cytochrome P450	55	2.7238	6	0.050712	1.2949	1	0.57957	0.1087
Steroid hormone biosynthesis	87	4.3086	8	0.061136	1.2137	1	0.58071	0.1903
Ether lipid metabolism	20	0.99048	3	0.072589	1.1391	1	0.58071	0
Fructose and mannose metabolism	20	0.99048	3	0.072589	1.1391	1	0.58071	0.09765
Caffeine metabolism	10	0.49524	2	0.084194	1.0747	1	0.60722	0.69231
Neomycin, kanamycin and gentamicin biosynthesis	2	0.099048	1	0.096625	1.0149	1	0.60722	0
Glycerophospholipid metabolism	36	1.7829	4	0.098674	1.0058	1	0.60722	0.09383
alpha-Linolenic acid metabolism	13	0.64381	2	0.13274	0.877	1	0.75852	0.33333
Ubiquinone and other terpenoid-quinone biosynthesis	18	0.89143	2	0.22293	0.65183	1	1	0.23077
Purine metabolism	70	3.4667	5	0.26305	0.57995	1	1	0.13487
Nitrogen metabolism	6	0.29714	1	0.26306	0.57994	1	1	0
Taurine and hypotaurine metabolism	8	0.39619	1	0.33453	0.47556	1	1	0
Amino sugar and nucleotide sugar metabolism	42	2.08	3	0.34557	0.46147	1	1	0
Ascorbate and aldarate metabolism	9	0.44571	1	0.36766	0.43456	1	1	0
Sphingolipid metabolism	32	1.5848	2	0.47679	0.32167	1	1	0.35835
Arginine biosynthesis	14	0.69333	1	0.51038	0.29211	1	1	0
D-Amino acid metabolism	15	0.74286	1	0.53484	0.27177	1	1	0
Retinol metabolism	17	0.8419	1	0.58021	0.23642	1	1	0.15464
Terpenoid backbone biosynthesis	18	0.89143	1	0.60123	0.22096	1	1	0.18254
Pantothenate and CoA biosynthesis	20	0.99048	1	0.64019	0.19369	1	1	0.0068
Glycolysis / Gluconeogenesis	26	1.2876	1	0.73591	0.13317	1	1	0.00944
Folate biosynthesis	27	1.3371	1	0.74921	0.1254	1	1	0
Alanine, aspartate and glutamate metabolism	28	1.3867	1	0.76185	0.11813	1	1	0.11378

Glutathione metabolism	28	1.3867	1	0.76185	0.11813	1	1	0.25596
Inositol phosphate metabolism	30	1.4857	1	0.78526	0.10498	1	1	0.12939
Glyoxylate and dicarboxylate metabolism	32	1.5848	1	0.8064	0.093447	1	1	0
Fatty acid elongation	39	1.9314	1	0.86545	0.062758	1	1	0
Fatty acid degradation	39	1.9314	1	0.86545	0.062758	1	1	0
Pyrimidine metabolism	39	1.9314	1	0.86545	0.062758	1	1	0
Tyrosine metabolism	42	2.08	1	0.88494	0.053087	1	1	0.00635
Primary bile acid biosynthesis	46	2.2781	1	0.90665	0.042562	1	1	0.05573
Fatty acid biosynthesis	47	2.3276	1	0.91141	0.040286	1	1	0.01473

*Metabolomic pathways significantly altered (FDR < 0.05) due to omitted LN_2 quenching are shown in red font. Cells were washed by ammonium formate, dried, and stored at -80℃ (48h).

Table S6. Pathway analysis of Group 1 vs. Group 3 SCMS results in the positive ion mode. *

Pathways	**Total**	**Expected**	**Hits**	**Raw p**	**-log10(p)**	**Holm adjust**	**FDR**	**Impact**
Metabolism of xenobiotics by cytochrome P450	68	0.47492	4	0.0008349	3.0784	0.066792	0.066792	0.09183
Biosynthesis of unsaturated fatty acids	36	0.25143	2	0.024549	1.61	1	0.98195	0
Purine metabolism	70	0.48889	2	0.082653	1.0827	1	1	0.00565
alpha-Linolenic acid metabolism	13	0.090794	1	0.087404	1.0585	1	1	0.33333
Glycerophospholipid metabolism	36	0.25143	1	0.22521	0.64741	1	1	0.01896
Steroid biosynthesis	41	0.28635	1	0.25254	0.59766	1	1	0
Primary bile acid biosynthesis	46	0.32127	1	0.279	0.5544	1	1	0.00016

* No metabolomic pathway was affected significantly (FDR < 0.05) by storage at -80°C (48h). Cells were washed, LN_2 quenched, and dried.

Table S7. Pathway analysis of Group 2 vs. Group 4 SCMS results in the positive ion mode. *

Pathways	Total	Expected	Hits	Raw p	-log10(p)	Holm adjust	FDR	Impact
Galactose metabolism	27	0.75429	11	2.042E-11	10.69	1.6336E-09	1.6336E-09	0.70254
Starch and sucrose metabolism	18	0.50286	7	2.0591E-07	6.6863	1.6267E-05	8.2362E-06	0.54856
Arachidonic acid metabolism	44	1.2292	5	0.006511	2.1864	0.50786	0.17363	0.02913
Fructose and mannose metabolism	20	0.55873	3	0.016643	1.7788	1	0.33286	0.09765
Caffeine metabolism	10	0.27937	2	0.029775	1.5262	1	0.47639	0.69231
Neomycin, kanamycin and gentamicin biosynthesis	2	0.055873	1	0.05511	1.2588	1	0.7348	0
Amino sugar and nucleotide sugar metabolism	42	1.1733	3	0.10977	0.9595	1	1	0
Nitrogen metabolism	6	0.16762	1	0.15657	0.80529	1	1	0
Drug metabolism - cytochrome P450	55	1.5365	3	0.19638	0.70689	1	1	0.02174
Taurine and hypotaurine metabolism	8	0.22349	1	0.20323	0.69202	1	1	0
Ascorbate and aldarate metabolism	9	0.25143	1	0.2256	0.64666	1	1	0
Glycerophospholipid metabolism	36	1.0057	2	0.26624	0.57473	1	1	0.05751
Pyrimidine metabolism	39	1.0895	2	0.29785	0.526	1	1	0.03985
alpha-Linolenic acid metabolism	13	0.36317	1	0.30911	0.50989	1	1	0
Purine metabolism	70	1.9556	3	0.3106	0.50779	1	1	0.00565
Steroid biosynthesis	41	1.1454	2	0.31885	0.49642	1	1	0.00346
Arginine biosynthesis	14	0.39111	1	0.32857	0.48337	1	1	0
D-Amino acid metabolism	15	0.41905	1	0.3475	0.45905	1	1	0
Primary bile acid biosynthesis	46	1.2851	2	0.37067	0.43101	1	1	0.11029
Ubiquinone and other terpenoid-quinone biosynthesis	18	0.50286	1	0.4012	0.39664	1	1	0.23077
Ether lipid metabolism	20	0.55873	1	0.43458	0.36193	1	1	0
Pantothenate and CoA biosynthesis	20	0.55873	1	0.43458	0.36193	1	1	0.0068
Glycolysis / Gluconeogenesis	26	0.72635	1	0.52417	0.28053	1	1	0.00944
Folate biosynthesis	27	0.75429	1	0.53768	0.26948	1	1	0
Alanine, aspartate and glutamate metabolism	28	0.78222	1	0.55082	0.25899	1	1	0.11378
Glutathione metabolism	28	0.78222	1	0.55082	0.25899	1	1	0.25596
Inositol phosphate metabolism	30	0.8381	1	0.57602	0.23956	1	1	0.12939

Glyoxylate and dicarboxylate metabolism	32	0.89397	1	0.59983	0.22197	1	1	0
Sphingolipid metabolism	32	0.89397	1	0.59983	0.22197	1	1	0.21576
Biosynthesis of unsaturated fatty acids	36	1.0057	1	0.6436	0.19138	1	1	0

*Metabolomic pathways significantly altered (FDR < 0.05) due to omitted LN_2 quenching are shown in red font. Cells were washed and dried.

Table S8. Pathway analysis of Group 1 vs. Group 2 SCMS results in the negative ion mode. *

Pathways	Total	Expected	Hits	Raw p	-log10(p)	Holm adjust	FDR	Impact
Galactose metabolism	27	0.44571	6	2.5748e-06	5.5893	0.000206	0.000206	0.42037
Fructose and mannose metabolism	20	0.33016	3	0.003782	2.4223	0.29877	0.10085	0.09765
Citrate cycle (TCA cycle)	20	0.33016	3	0.003782	2.4223	0.29877	0.10085	0.16809
Alanine, aspartate and glutamate metabolism	28	0.46222	3	0.009955	2.002	0.76651	0.174	0
Caffeine metabolism	10	0.16508	2	0.010875	1.9636	0.82649	0.174	0.69231
Histidine metabolism	16	0.26413	2	0.027289	1.564	1	0.30309	0.04918
Amino sugar and nucleotide sugar metabolism	42	0.69333	3	0.029932	1.5239	1	0.30309	0
Neomycin, kanamycin and gentamicin biosynthesis	2	0.033016	1	0.032754	1.4847	1	0.30309	0
Starch and sucrose metabolism	18	0.29714	2	0.034098	1.4673	1	0.30309	0.42527
Glyoxylate and dicarboxylate metabolism	32	0.52825	2	0.096066	1.0174	1	0.7167	0.03175
Metabolism of xenobiotics by cytochrome P450	68	1.1225	3	0.098546	1.0064	1	0.7167	0
Pyrimidine metabolism	39	0.64381	2	0.13389	0.87325	1	0.79692	0.08894
Drug metabolism - other enzymes	39	0.64381	2	0.13389	0.87325	1	0.79692	0.13043
Ascorbate and aldarate metabolism	9	0.14857	1	0.13946	0.85555	1	0.79692	0
Butanoate metabolism	15	0.24762	1	0.22183	0.65398	1	1	0

Nicotinate and nicotinamide metabolism	15	0.24762	1	0.22183	0.65398	1	1	0
Pantothenate and CoA biosynthesis	20	0.33016	1	0.28463	0.54572	1	1	0
beta-Alanine metabolism	21	0.34667	1	0.29659	0.52784	1	1	0
Propanoate metabolism	22	0.36317	1	0.30836	0.51094	1	1	0
Glycolysis / Gluconeogenesis	26	0.42921	1	0.35357	0.45152	1	1	0.00944
Inositol phosphate metabolism	30	0.49524	1	0.39593	0.40238	1	1	0.12939
Valine, leucine and isoleucine degradation	40	0.66032	1	0.49048	0.30938	1	1	0.02264
Arachidonic acid metabolism	44	0.72635	1	0.52417	0.28053	1	1	0
Purine metabolism	70	1.1556	1	0.6963	0.1572	1	1	0.01146
Steroid hormone biosynthesis	87	1.4362	1	0.77453	0.11096	1	1	0

*Metabolomic pathways significantly altered (FDR < 0.05) due to omitted LN_2 quenching are shown in red font. Cells were washed and dried.

Table S9. Pathway analysis of Group 3 vs. Group 4 SCMS results in the negative ion mode. *

Pathways	Total	Expected	Hits	Raw p	-log10(p)	Holm adjust	FDR	Impact
Alanine, aspartate and glutamate metabolism	28	1.9733	11	1.0159E-06	5.9931	8.1276E-05	8.085E-05	0.75562
D-Amino acid metabolism	15	1.0571	8	2.0212E-06	5.6944	0.00015968	8.085E-05	1
Butanoate metabolism	15	1.0571	7	2.8803E-05	4.5406	0.0022466	0.00076807	0.17461
Linoleic acid metabolism	5	0.35238	4	0.00011085	3.9553	0.0085355	0.002217	1
Galactose metabolism	27	1.9029	8	0.00033944	3.4692	0.025798	0.0054311	0.42037
Arginine and proline metabolism	36	2.5371	9	0.00058114	3.2357	0.043586	0.0077486	0.15697
Valine, leucine and isoleucine biosynthesis	8	0.56381	4	0.0013127	2.8818	0.097137	0.013182	0
Valine, leucine and isoleucine degradation	40	2.819	9	0.0013271	2.8771	0.097137	0.013182	0.09069
Glycine, serine and threonine metabolism	33	2.3257	8	0.001483	2.8289	0.10677	0.013182	0.3839

Pantothenate and CoA biosynthesis	20	1.4095	6	0.0018358	2.7362	0.13034	0.014686	0.12245
Caffeine metabolism	10	0.70476	4	0.0035241	2.453	0.24668	0.02563	0.69231
beta-Alanine metabolism	21	1.48	5	0.012985	1.8866	0.89597	0.086567	0.5597
Propanoate metabolism	22	1.5505	5	0.015879	1.7992	1	0.095215	0.04103
Pyrimidine metabolism	39	2.7486	7	0.016663	1.7783	1	0.095215	0.12673
Histidine metabolism	16	1.1276	4	0.021952	1.6585	1	0.11708	0.04918
Phenylalanine, tyrosine and tryptophan biosynthesis	4	0.2819	2	0.026892	1.5704	1	0.13446	1
Fructose and mannose metabolism	20	1.4095	4	0.047012	1.3278	1	0.22124	0.13078
Nitrogen metabolism	6	0.42286	2	0.061245	1.2129	1	0.2722	0
Arginine biosynthesis	14	0.98667	3	0.070106	1.1542	1	0.29518	0.11675
Nicotinate and nicotinamide metabolism	15	1.0571	3	0.083285	1.0794	1	0.33314	0
Biosynthesis of unsaturated fatty acids	36	2.5371	5	0.10401	0.98291	1	0.37914	0
Phenylalanine metabolism	8	0.56381	2	0.10426	0.98187	1	0.37914	0.35714
Drug metabolism - other enzymes	39	2.7486	5	0.13474	0.87051	1	0.45342	0.20651
Neomycin, kanamycin and gentamicin biosynthesis	2	0.14095	1	0.13603	0.86637	1	0.45342	0
Glyoxylate and dicarboxylate metabolism	32	2.2552	4	0.18424	0.73462	1	0.58957	0.04233
Metabolism of xenobiotics by cytochrome P450	68	4.7924	6	0.34508	0.46208	1	1	0
Starch and sucrose metabolism	18	1.2686	2	0.36586	0.43669	1	1	0.42527
Arachidonic acid metabolism	44	3.101	4	0.37621	0.42458	1	1	0.34609
Cysteine and methionine metabolism	33	2.3257	3	0.41461	0.38237	1	1	0.12346
Citrate cycle (TCA cycle)	20	1.4095	2	0.41735	0.3795	1	1	0.07685

Taurine and hypotaurine metabolism	8	0.56381	1	0.44346	0.35315	1	1	0.42857
Ascorbate and aldarate metabolism	9	0.63429	1	0.48288	0.31616	1	1	0
Purine metabolism	70	4.9333	5	0.55744	0.2538	1	1	0.09122
Folate biosynthesis	27	1.9029	2	0.57855	0.23766	1	1	0.09924
Amino sugar and nucleotide sugar metabolism	42	2.96	3	0.5786	0.23762	1	1	0
Tyrosine metabolism	42	2.96	3	0.5786	0.23762	1	1	0.13972
Glutathione metabolism	28	1.9733	2	0.59879	0.22273	1	1	0.04258
Primary bile acid biosynthesis	46	3.2419	3	0.64179	0.1926	1	1	0.00774
Porphyrin metabolism	31	2.1848	2	0.65514	0.18367	1	1	0.02795
Retinol metabolism	17	1.1981	1	0.71321	0.14678	1	1	0.15464
Ubiquinone and other terpenoid-quinone biosynthesis	18	1.2686	1	0.73364	0.13452	1	1	0
Terpenoid backbone biosynthesis	18	1.2686	1	0.73364	0.13452	1	1	0.11429
Pentose and glucuronate interconversions	19	1.339	1	0.75263	0.12342	1	1	0
Selenocompound metabolism	20	1.4095	1	0.77028	0.11335	1	1	0
Ether lipid metabolism	20	1.4095	1	0.77028	0.11335	1	1	0
Tryptophan metabolism	41	2.8895	2	0.7986	0.097669	1	1	0.03184
Pyruvate metabolism	23	1.621	1	0.81607	0.088272	1	1	0.0283
Glycolysis / Gluconeogenesis	26	1.8324	1	0.8528	0.069152	1	1	0.00944
Lipoic acid metabolism	28	1.9733	1	0.87315	0.058912	1	1	0.06136
Inositol phosphate metabolism	30	2.1143	1	0.8907	0.050266	1	1	0.12939
Lysine degradation	30	2.1143	1	0.8907	0.050266	1	1	0.13429
Sphingolipid metabolism	32	2.2552	1	0.90585	0.042944	1	1	0
Drug metabolism - cytochrome P450	55	3.8762	2	0.91103	0.040466	1	1	0.01449

Glycerophospholipid metabolism	36	2.5371	1	0.93018	0.031434	1	1	0.04289
Steroid biosynthesis	41	2.8895	1	0.952	0.021362	1	1	0
Fatty acid biosynthesis	47	3.3124	1	0.96944	0.01348	1	1	0

*Metabolomic pathways significantly altered (FDR < 0.05) due to omitted LN_2 quenching are shown in red font. Cells were washed, dried, and stored at -80℃ (48h).

Table S10. Pathway analysis of Group 1 vs. Group 3 SCMS results in the negative ion mode.*

Pathways	Total	Expected	Hits	Raw p	-log10(p)	Holm adjust	FDR	Impact
Arachidonic acid metabolism	44	2.5422	15	4.9516E-09	8.3053	3.9613E-07	3.9613E-07	0.27518
Arginine and proline metabolism	36	2.08	10	1.8508E-05	4.7326	0.0014621	0.00074032	0.18023
Linoleic acid metabolism	5	0.28889	4	5.0001E-05	4.301	0.0039001	0.0013334	1
D-Amino acid metabolism	15	0.86667	6	0.00010365	3.9844	0.0079809	0.002073	1
Valine, leucine and isoleucine biosynthesis	8	0.46222	4	0.00061128	3.2138	0.046457	0.0084496	0
Pantothenate and CoA biosynthesis	20	1.1556	6	0.00063372	3.1981	0.047529	0.0084496	0.12245
Alanine, aspartate and glutamate metabolism	28	1.6178	7	0.00074502	3.1278	0.055131	0.0085145	0.48398
Galactose metabolism	27	1.56	6	0.0034808	2.4583	0.2541	0.034808	0.42037
Glycine, serine and threonine metabolism	33	1.9067	6	0.009832	2.0074	0.7079	0.087395	0.2208
Biosynthesis of unsaturated fatty acids	36	2.08	6	0.015031	1.823	1	0.12025	0
Phenylalanine, tyrosine and tryptophan biosynthesis	4	0.23111	2	0.018358	1.7362	1	0.13351	1
Pyrimidine metabolism	39	2.2533	6	0.021895	1.6597	1	0.14597	0.0904
beta-Alanine metabolism	21	1.2133	4	0.029267	1.5336	1	0.18011	0.5597
Nitrogen metabolism	6	0.34667	2	0.042536	1.3712	1	0.24306	0

Butanoate metabolism	15	0.86667	3	0.051207	1.2907	1	0.2731	0.03175
Phenylalanine metabolism	8	0.46222	2	0.07364	1.1329	1	0.36001	0.35714
Valine, leucine and isoleucine degradation	40	2.3111	5	0.076503	1.1163	1	0.36001	0
Fructose and mannose metabolism	20	1.1556	3	0.10438	0.98139	1	0.42763	0.09765
Glyoxylate and dicarboxylate metabolism	32	1.8489	4	0.10885	0.96319	1	0.42763	0.03175
Caffeine metabolism	10	0.57778	2	0.10984	0.95922	1	0.42763	0.69231
Neomycin, kanamycin and gentamicin biosynthesis	2	0.11556	1	0.11225	0.94981	1	0.42763	0
Arginine biosynthesis	14	0.80889	2	0.19178	0.71719	1	0.69739	0.11675
Drug metabolism - cytochrome P450	55	3.1778	5	0.20813	0.68166	1	0.72394	0.03623
Starch and sucrose metabolism	18	1.04	2	0.27925	0.55401	1	0.93083	0.42527
Citrate cycle (TCA cycle)	20	1.1556	2	0.3231	0.49066	1	1	0.13536
Taurine and hypotaurine metabolism	8	0.46222	1	0.37949	0.4208	1	1	0.42857
Ascorbate and aldarate metabolism	9	0.52	1	0.41552	0.38141	1	1	0
Amino sugar and nucleotide sugar metabolism	42	2.4267	3	0.44186	0.35472	1	1	0
Folate biosynthesis	27	1.56	2	0.46898	0.32884	1	1	0.09924
Glutathione metabolism	28	1.6178	2	0.48836	0.31126	1	1	0.02675
Primary bile acid biosynthesis	46	2.6578	3	0.5031	0.29835	1	1	0.00774
alpha-Linolenic acid metabolism	13	0.75111	1	0.5401	0.26753	1	1	0.33333
Porphyrin metabolism	31	1.7911	2	0.5438	0.26456	1	1	0.02795
Nicotinate and nicotinamide metabolism	15	0.86667	1	0.59214	0.22758	1	1	0
Histidine metabolism	16	0.92444	1	0.61593	0.21047	1	1	0

Ubiquinone and other terpenoid-quinone biosynthesis	18	1.04	1	0.65947	0.1808	1	1	0
Pentose and glucuronate interconversions	19	1.0978	1	0.67937	0.16789	1	1	0
Selenocompound metabolism	20	1.1556	1	0.69813	0.15607	1	1	0
Propanoate metabolism	22	1.2711	1	0.73243	0.13523	1	1	0
Purine metabolism	70	4.0444	3	0.78354	0.10594	1	1	0.01146
Glycolysis / Gluconeogenesis	26	1.5022	1	0.7899	0.10243	1	1	0.00944
Lysine degradation	30	1.7333	1	0.83513	0.078247	1	1	0.11247
Inositol phosphate metabolism	30	1.7333	1	0.83513	0.078247	1	1	0.12939
Cysteine and methionine metabolism	33	1.9067	1	0.86259	0.064193	1	1	0.04179
Fatty acid elongation	39	2.2533	1	0.90467	0.043511	1	1	0
Fatty acid degradation	39	2.2533	1	0.90467	0.043511	1	1	0
Drug metabolism - other enzymes	39	2.2533	1	0.90467	0.043511	1	1	0
Steroid biosynthesis	41	2.3689	1	0.91563	0.038279	1	1	0
Tyrosine metabolism	42	2.4267	1	0.92064	0.035911	1	1	0.13972
Fatty acid biosynthesis	47	2.7156	1	0.94158	0.026142	1	1	0.01473
Metabolism of xenobiotics by cytochrome P450	68	3.9289	1	0.98405	0.0069824	1	1	0.05612

*Metabolomic pathways significantly altered (FDR < 0.05) due to storage at -80°C (48h) are shown in red font. Cells were washed by ammonium formate, quenched by LN_2, and freeze-dried in a vacuum.

Table S11. Pathway analysis of Group 2 vs. Group 4 SCMS results in the negative ion mode. *

	Total	Expected	Hits	Raw p	-log10(p)	Holm adjust	FDR	Impact
Arachidonic acid metabolism	44	2.6819	16	1.0783E-09	8.9673	8.6263E-08	8.6263E-08	0.27518
Valine, leucine and isoleucine biosynthesis	8	0.48762	4	0.00075176	3.1239	0.059389	0.021719	0
Galactose metabolism	27	1.6457	7	0.00081447	3.0891	0.063529	0.021719	0.45614
Biosynthesis of unsaturated fatty acids	36	2.1943		0.0048618	2.3132	0.37436	0.097236	0
Arginine and proline metabolism	36	2.1943	6	0.019229	1.716	1	0.27138	0.1093
Phenylalanine, tyrosine and tryptophan biosynthesis	4	0.24381	2	0.020353	1.6914	1	0.27138	1
Alanine, aspartate and glutamate metabolism	28	1.7067	5	0.024295	1.6145	1	0.27766	0.08654
Pantothenate and CoA biosynthesis	20	1.219	4	0.029529	1.5298	1	0.29529	0.05442
Glycine, serine and threonine metabolism	33	2.0114	5	0.04614	1.3359	1	0.41013	0.14654
D-Amino acid metabolism	15	0.91429	3	0.058508	1.2328	1	0.46807	0
Phenylalanine metabolism	8	0.48762	2	0.080952	1.0918	1	0.56591	0.35714
Drug metabolism - cytochrome P450	55	3.3524	6	0.11329	0.94583	1	0.56591	0.03623
Metabolism of xenobiotics by cytochrome P450	68	4.1448	7	0.115	0.93929	1	0.56591	0.05612
Fructose and mannose metabolism	20	1.219	3	0.11792	0.92842	1	0.56591	0.09765
Citrate cycle (TCA cycle)	20	1.219	3	0.11792	0.92842	1	0.56591	0.16809
Neomycin, kanamycin and gentamicin biosynthesis	2	0.1219	1	0.11823	0.92729	1	0.56591	0
Caffeine metabolism	10	0.60952	2	0.12026	0.91989	1	0.56591	0.69231
Pyrimidine metabolism	39	2.3771	4	0.21046	0.67682	1	0.93539	0.09684
Valine, leucine and isoleucine degradation	40	2.4381	4	0.22366	0.65041	1	0.94173	0.02264

Histidine metabolism	16	0.97524	2	0.25455	0.59423	1	1	0.04918
Linoleic acid metabolism	5	0.30476	1	0.27011	0.56846	1	1	1
Starch and sucrose metabolism	18	1.0971	2	0.30103	0.5214	1	1	0.42527
Fatty acid biosynthesis	47	2.8648	4	0.32075	0.49383	1	1	0.01473
beta-Alanine metabolism	21	1.28	2	0.3697	0.43215	1	1	0.39925
Propanoate metabolism	22	1.341	2	0.39205	0.40665	1	1	0
Taurine and hypotaurine metabolism	8	0.48762	1	0.39605	0.40225	1	1	0.42857
Drug metabolism - other enzymes	39	2.3771	3	0.42846	0.36809	1	1	0.16847
Ascorbate and aldarate metabolism	9	0.54857	1	0.43305	0.36346	1	1	0
Amino sugar and nucleotide sugar metabolism	42	2.56	3	0.4777	0.32084	1	1	0
Folate biosynthesis	27	1.6457	2	0.49782	0.30293	1	1	0.09924
Primary bile acid biosynthesis	46	2.8038	3	0.54019	0.26745	1	1	0.00774
Lysine degradation	30	1.8286	2	0.55551	0.25531	1	1	0.24676
alpha-Linolenic acid metabolism	13	0.79238	1	0.55992	0.25188	1	1	0.33333
Glyoxylate and dicarboxylate metabolism	32	1.9505	2	0.59133	0.22817	1	1	0.03175
Butanoate metabolism	15	0.91429	1	0.61237	0.21299	1	1	0
Nicotinate and nicotinamide metabolism	15	0.91429	1	0.61237	0.21299	1	1	0
Ubiquinone and other terpenoid-quinone biosynthesis	18	1.0971	1	0.67966	0.16771	1	1	0
Terpenoid backbone biosynthesis	18	1.0971	1	0.67966	0.16771	1	1	0.11429
Selenocompound metabolism	20	1.219	1	0.71795	0.1439	1	1	0
Ether lipid metabolism	20	1.219	1	0.71795	0.1439	1	1	0
Glycolysis / Gluconeogenesis	26	1.5848	1	0.80769	0.092754	1	1	0.00944
Lipoic acid metabolism	28	1.7067	1	0.8308	0.080505	1	1	0.06136
Inositol phosphate metabolism	30	1.8286	1	0.85115	0.069993	1	1	0.12939

Porphyrin metabolism	31	1.8895	1	0.8604	0.065299	1	1	0.02795
Glycerophospholipid metabolism	36	2.1943	1	0.89877	0.04635	1	1	0.04289
Fatty acid elongation	39	2.3771	1	0.91657	0.037835	1	1	0
Fatty acid degradation	39	2.3771	1	0.91657	0.037835	1	1	0
Steroid biosynthesis	41	2.499	1	0.92668	0.033072	1	1	0
Tyrosine metabolism	42	2.56	1	0.93126	0.030927	1	1	0.13972
Purine metabolism	70	4.2667	2	0.93626	0.028604	1	1	0.01146
Steroid hormone biosynthesis	87	5.3029	1	0.99642	0.0015588	1	1	0

*Metabolomic pathways significantly altered (FDR < 0.05) due to storage at -80°C (48h) without LN_2 quenching are shown in red font. Cells were washed by ammonium formate and freeze-dried in a vacuum.

Supporting Figures

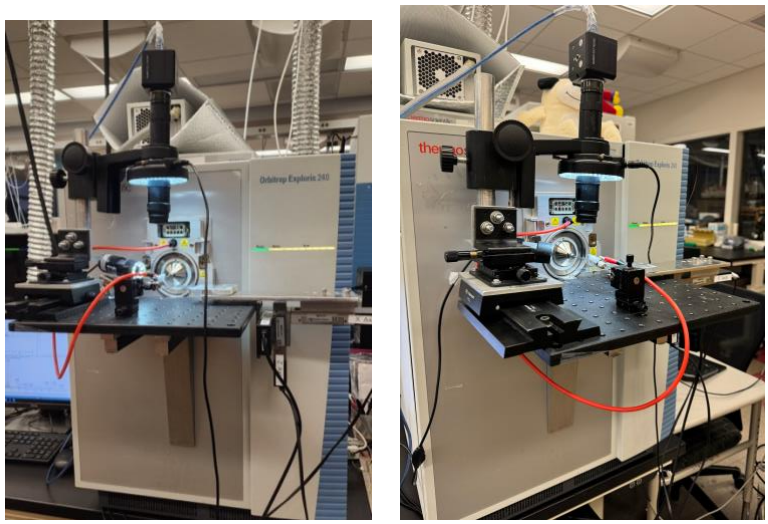

Figure S1. The Single-probe device coupled to Thermo Orbitrap Exploris 240 Mass Spectrometer for SCMS experiments.

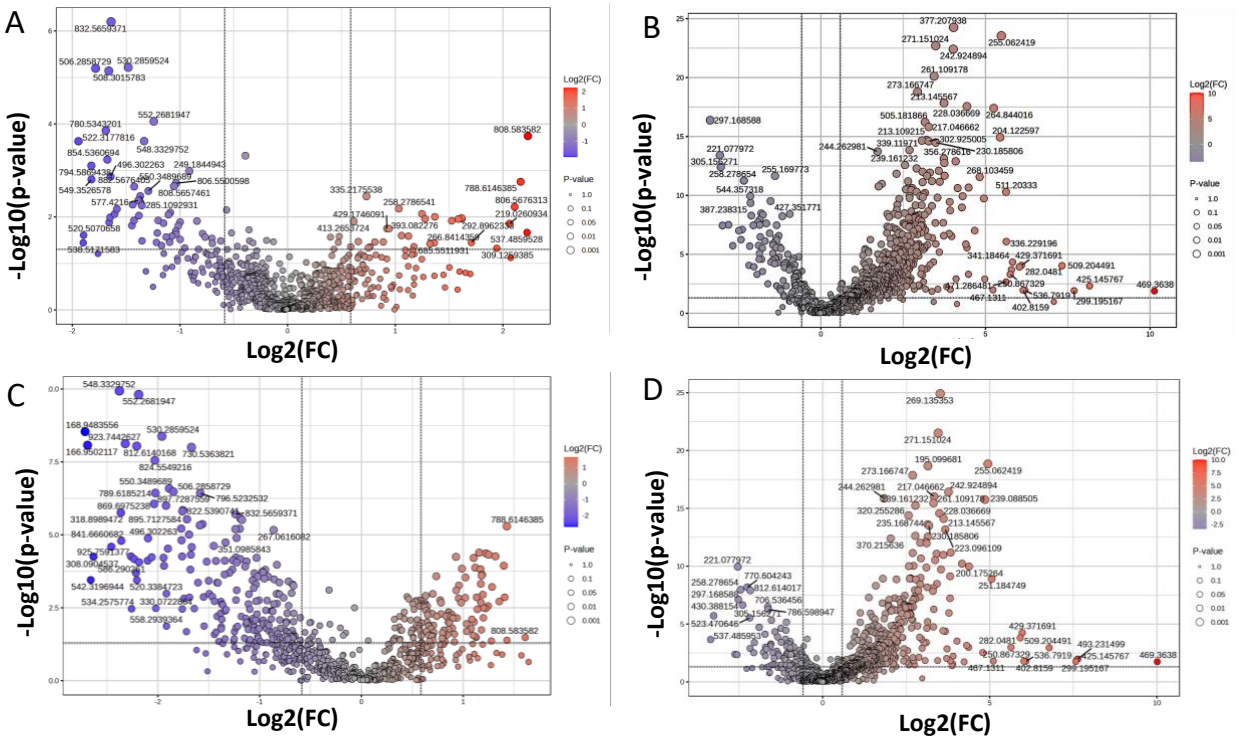

Figure S2. Volcano plots illustrating significantly changed species (fold change > 1.5 and p-value < 0.05) in the positive ion mode through pairwise comparison. **(A)** Group 1 vs. Group 2 (22 increased and 38 decreased metabolites), **(B)** Group 3 vs. Group 4 (324 increased and 53 decreased metabolites). **(C)** Group 1 vs. Group 3 (58 increased and 134 decreased metabolites). **(D)** Group 2 vs. Group 4 (144 increased and 100 decreased metabolites).

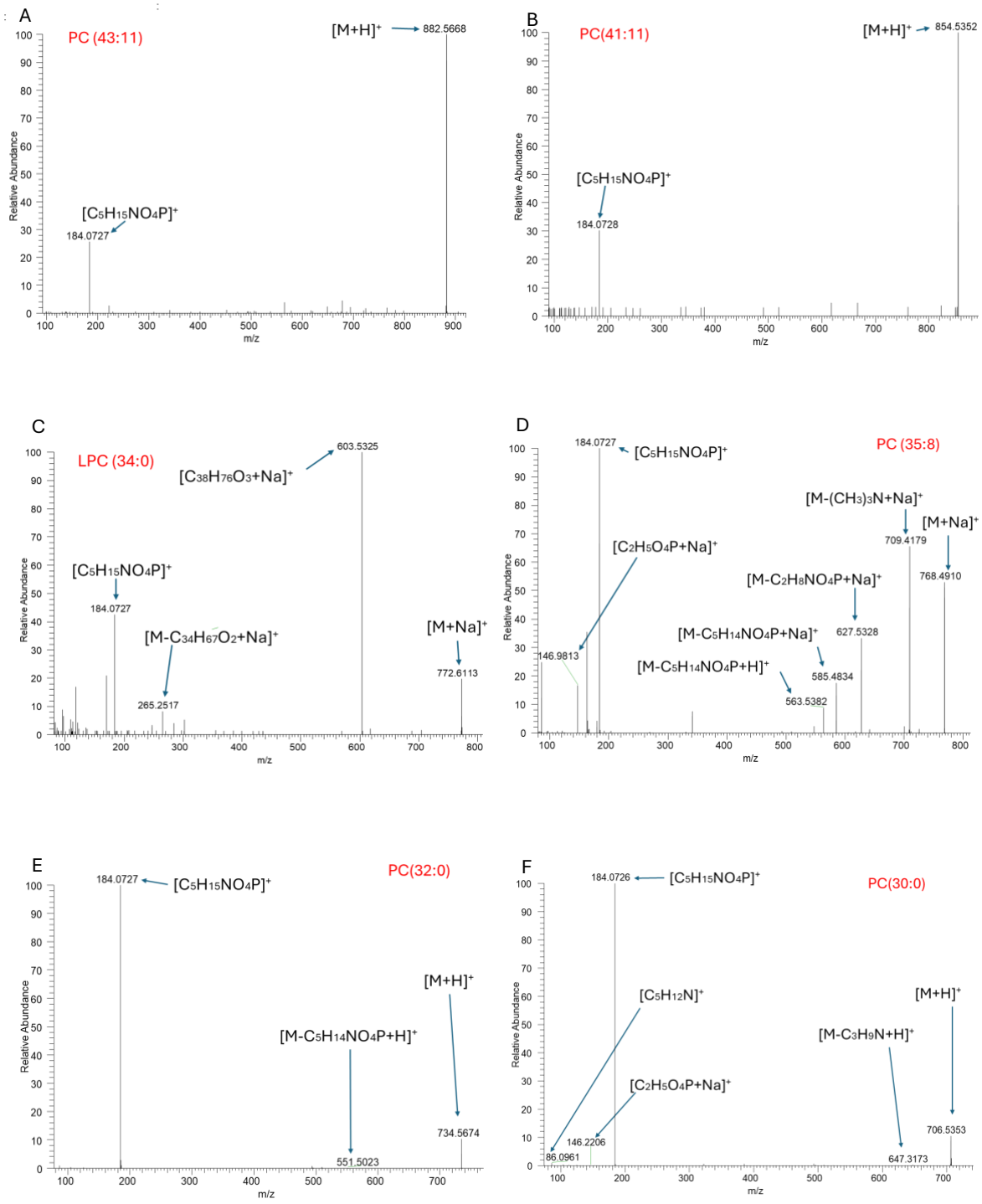

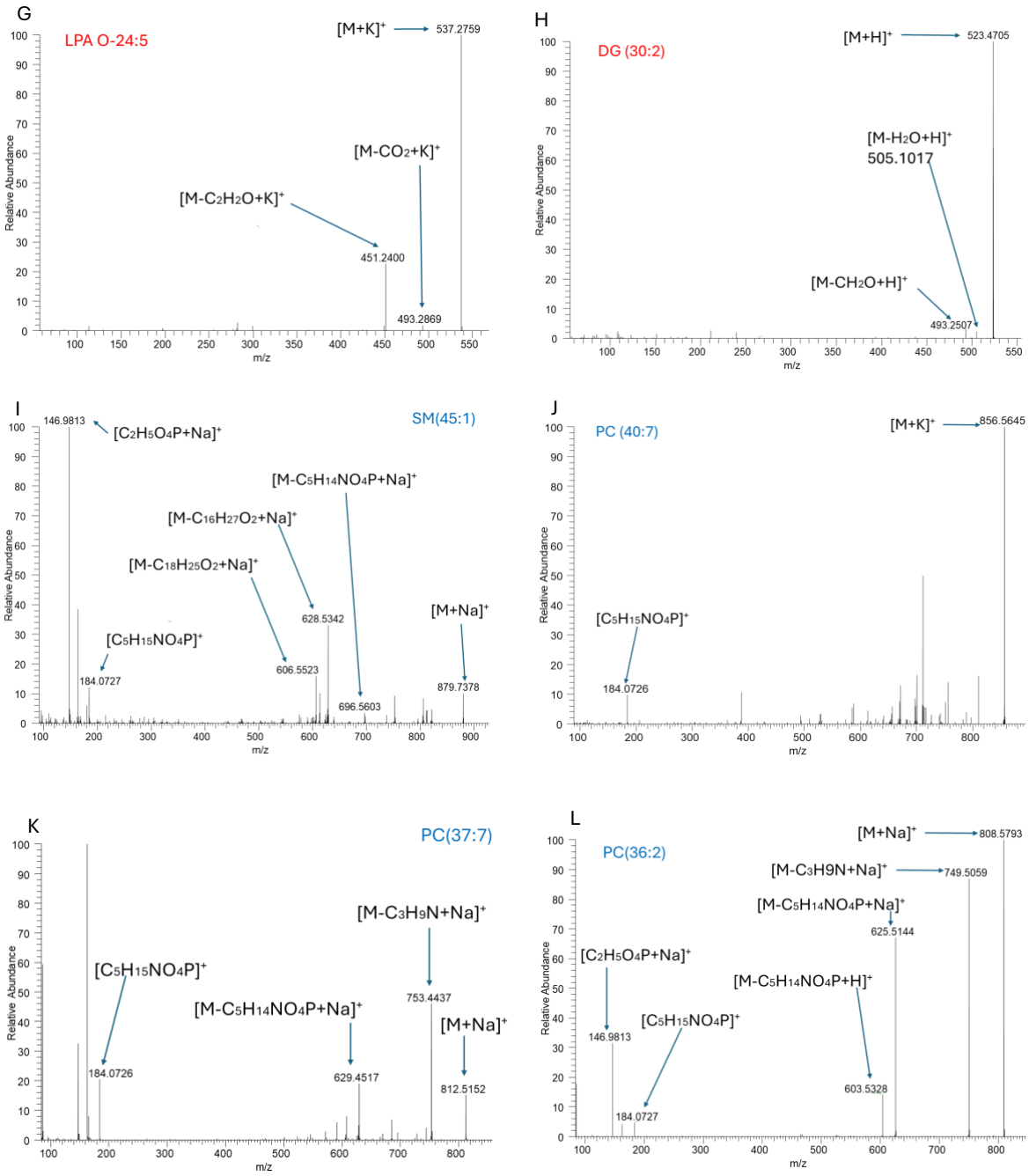

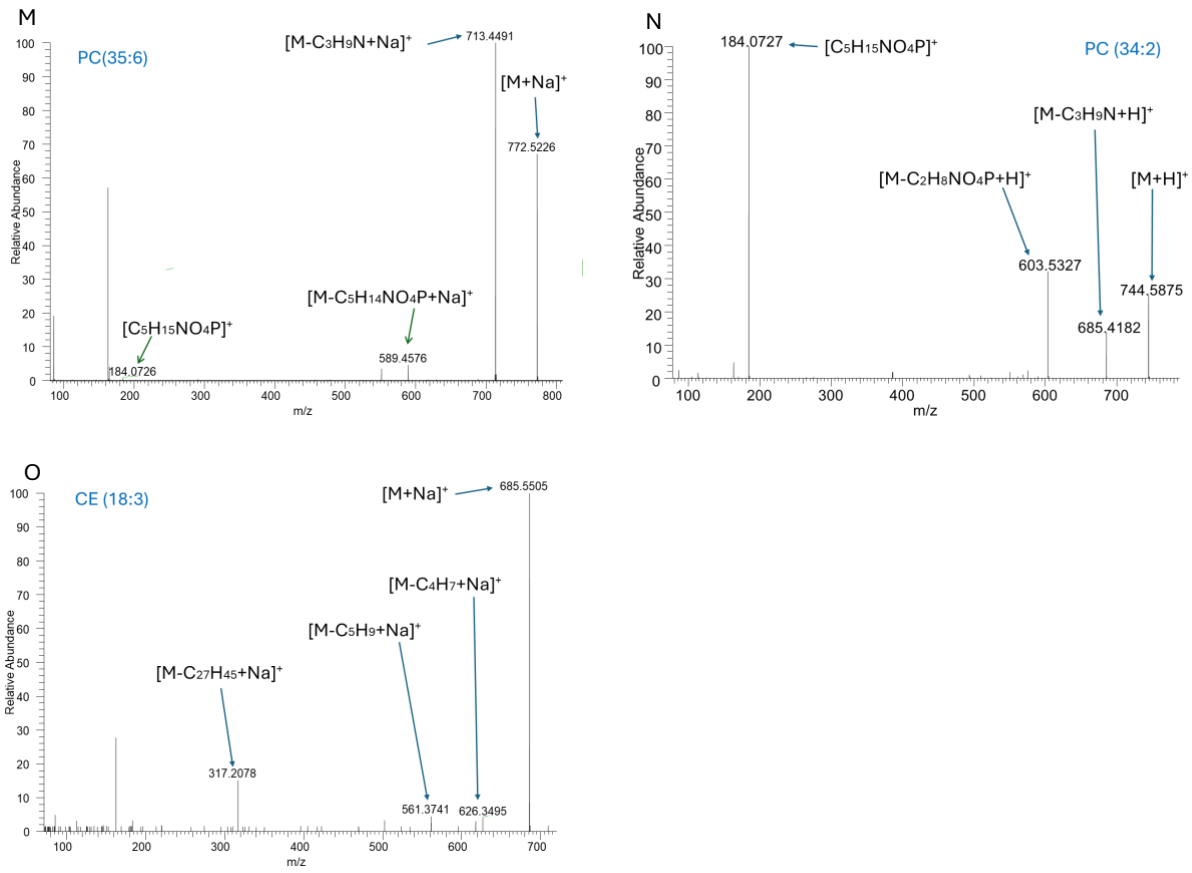

Figure S3. MS2 identification of metabolites in the positive ion mode at the single-cell level (cells in Group 4). (A) PC (43:11), (B) PC (41:11), (C) LPC (34:0), (D) PC(35:8), (E) PC(32:0), (F) PC(30:0), (G) LPA(24:5) and (H) DG(30:2), (I) SM(45:1), (J) PC(40:7), (K) PC(37:7), (L) PC(36:2), (M) PC(35:6), (N) PC(34:2), and (O) CE (18:3). (SM: sphingomylins; PC: phosphatidylcholine; LPC: lyso phosphatidylcholine; LPA: lysophosphatidic acid; DG: diglycerides CE: cholesteryl esters).

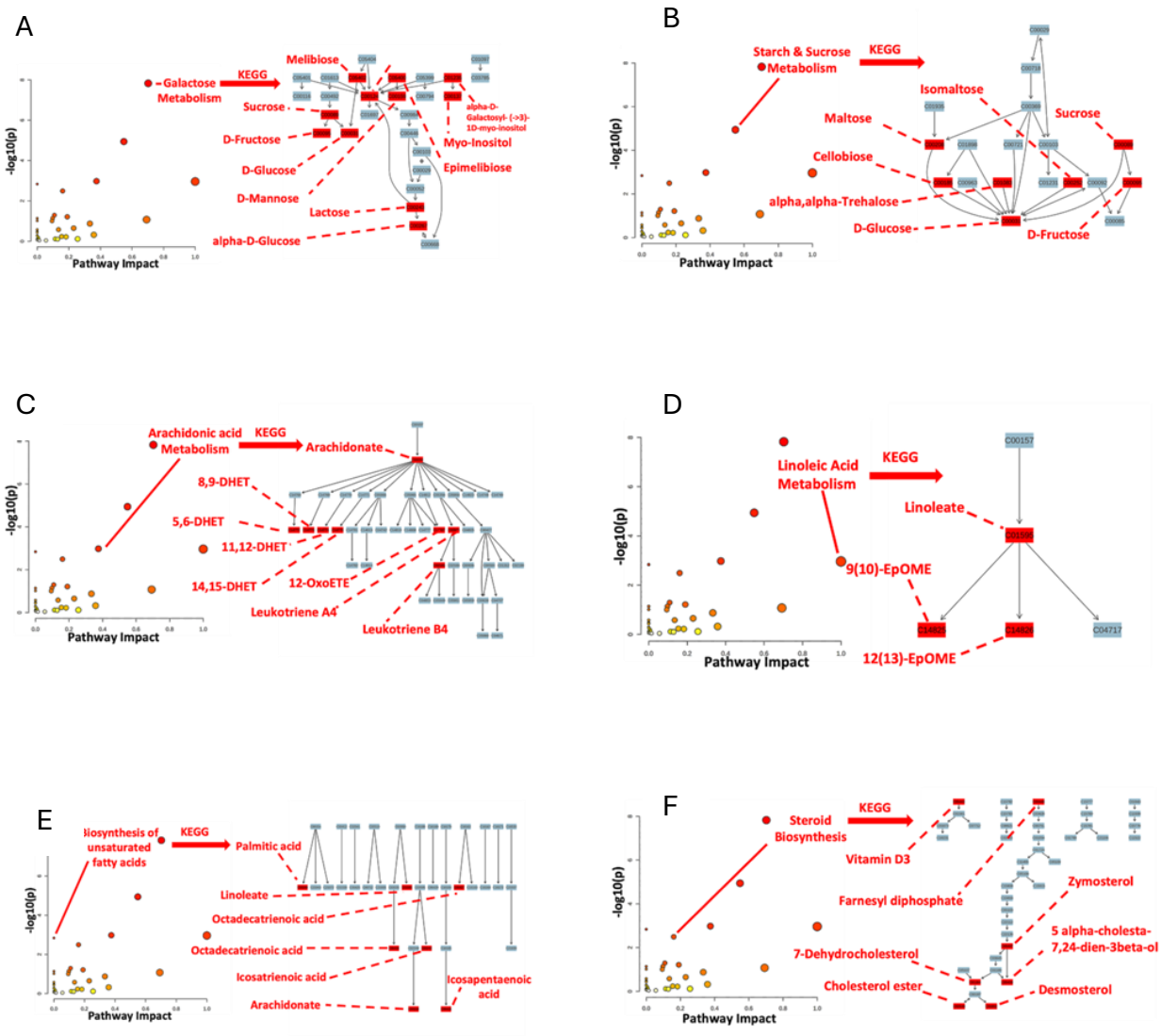

Figure S4. Pathway analysis using significantly changed metabolites ($p<0.05$ and FC > 1.5) from the comparison between Group 3 and Group 4 in the positive ion mode. **(A)** Galactose metabolism (FDR = 1.19E-6). **(B)** Starch and sucrose metabolism (FDR = 4.58E-4). **(C)** Arachidonic acid metabolism (FDR = 0.0218). **(D)** Linoleic acid metabolism (FDR = 0.0218). **(E)** Biosynthesis of unsaturated fatty acids pathway (FDR = 0.0233). **(F)** Steroid biosynthesis pathway (FDR = 0.0427). Identified (based on MS/MS) and tentatively labeled (based on comparison of accurate m/z and database) metabolites are shown in red font.

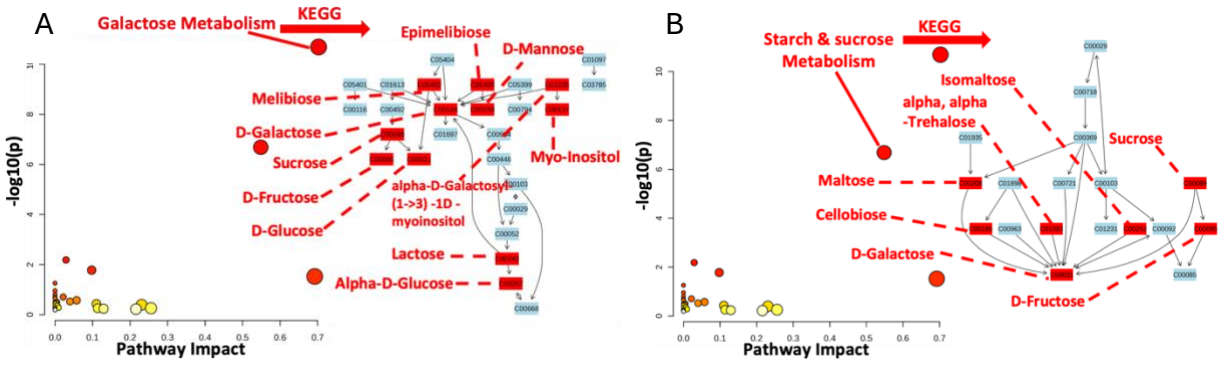

Figure S5. Pathway analysis using significantly changed metabolites (p<0.05 and FC > 1.5) from the comparison between Group 2 and Group 4 in the positive ion mode. **(A)** Galactose metabolism (FDR = 1.63 x 10^{-9}). **(B)** Starch and sucrose metabolism (FDR = = 8.24 x 10^{-6}). Identified (based on MS/MS) and tentatively labeled (based on comparison of accurate m/z and database) metabolites are shown in red font.

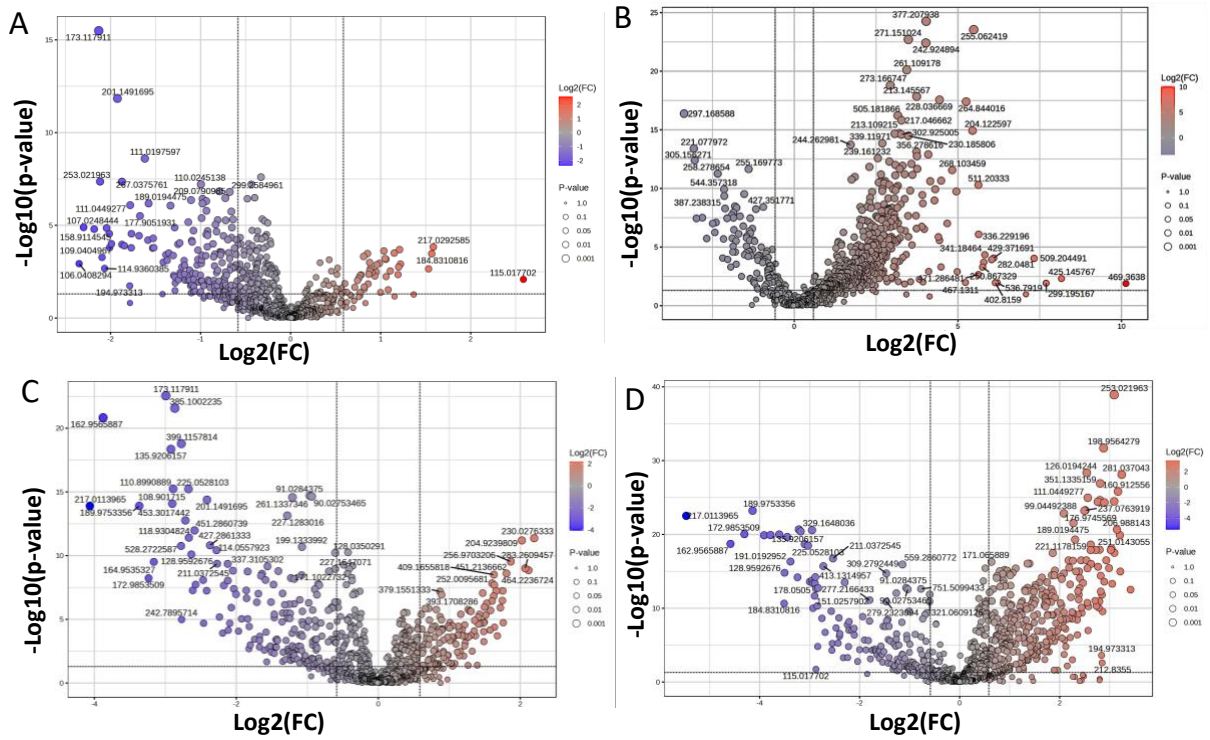

Figure S6. Volcano plots illustrating significantly changed species (fold change > 1.5 and p-value < 0.05) in the negative ion mode through pairwise comparison. **(A)** Group 1 vs. Group 2 (20 increased and 125 decreased metabolites). **(B)** Group 3 vs. Group 4 (235 increased and 56 decreased). **(C)** Group 1 vs. Group 3 (86 increased and 141 decreased metabolites). **(D)** Group 2 vs. Group 4 (87 increased and 187 decreased metabolites).

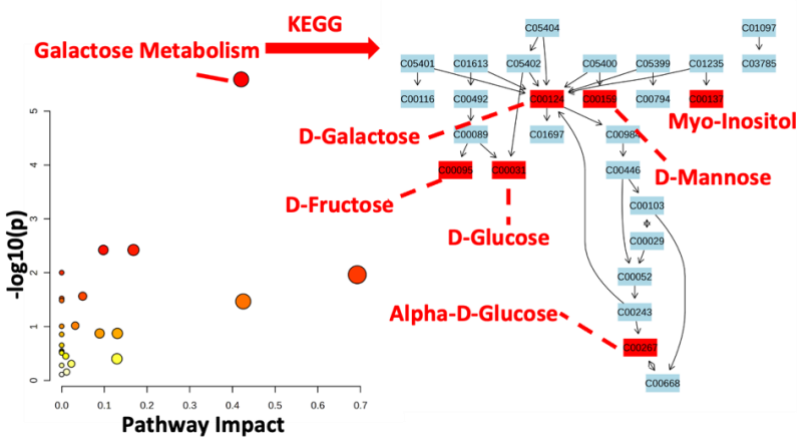

Figure S7. Pathway analysis using significantly changed metabolites ($p<0.05$ and FC > 1.5) from the comparison between Group 1 and Group 2 in the negative ion mode. Pathway analysis revealed that galactose metabolism (FDR = 2.06 x 10-4) significantly changed. Identified (based on MS/MS) and tentatively labeled (based on comparison of accurate m/z and database) metabolites are shown in red font.

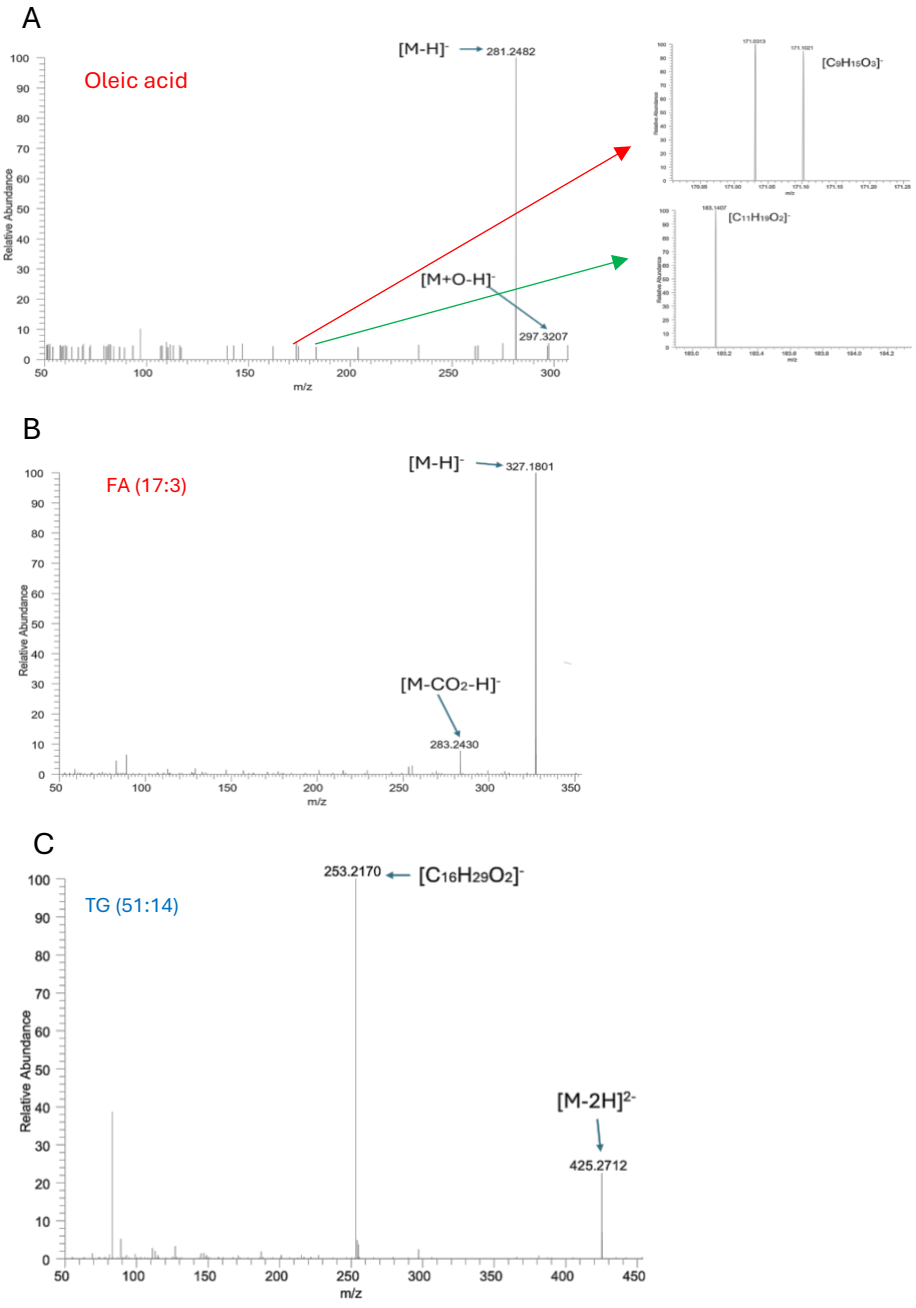

Figure S8. MS2 identification of metabolite in Group 4 cells using the Single-probe SCMS technique in negative mode. (A) Oleic acid FA (18:1), (B) FA (17:3) and (C)TG (51:14) (FA: fatty acids; TG: triglycerides).

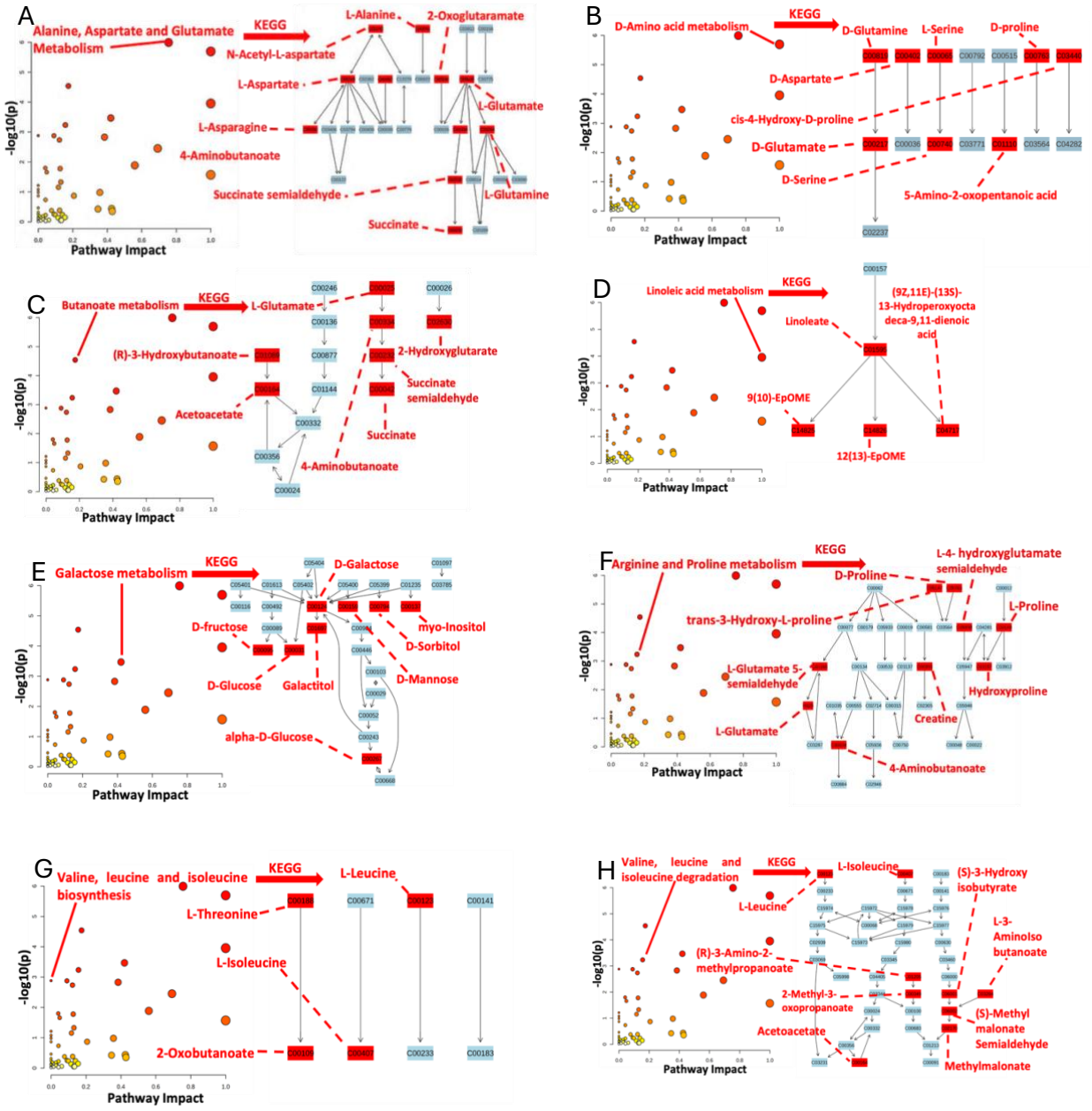

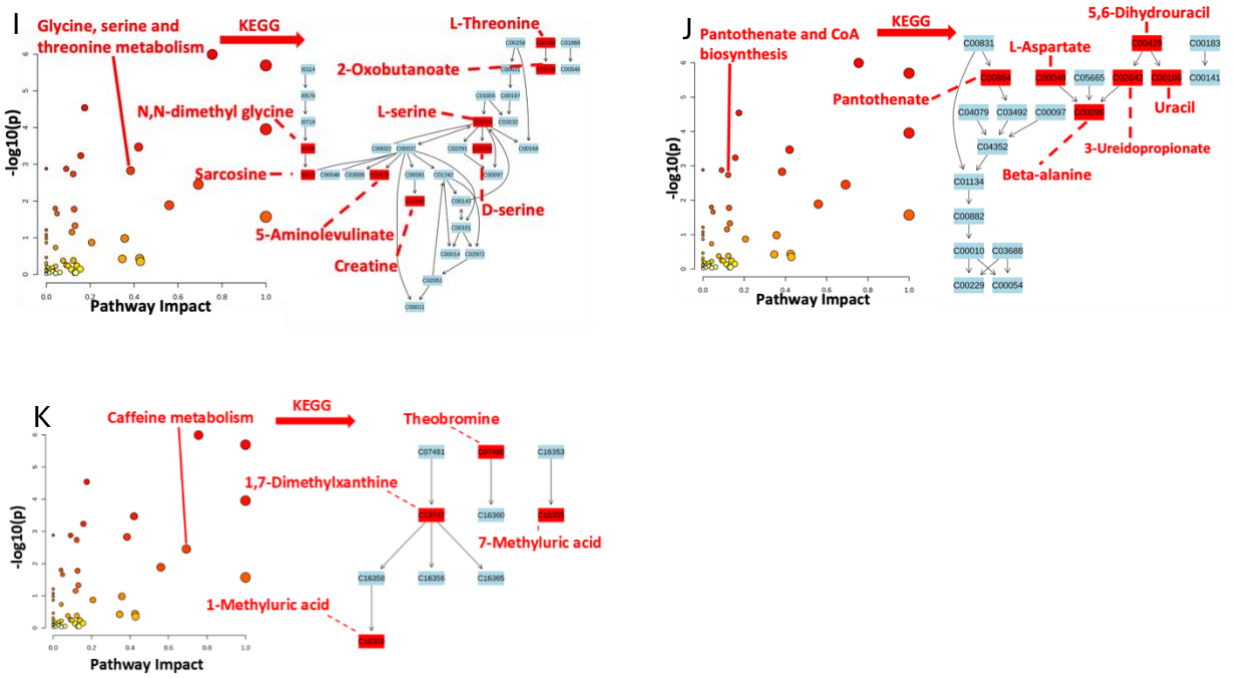

Figure S9. Pathway analysis using significantly changed metabolites ($p<0.05$ and FC > 1.5) from the comparison between Group 3 and Group 4 in the negative ion mode. **(A)** Alanine, aspartate, and glutamate metabolism, showing a highly significant association (FDR = 8.09E-05). **(B)** D-amino acid metabolism (FDR = 8.09E-05). **(C)** Butanoate metabolism pathway (FDR = 0.000768). **(D)** linoleic acid metabolism pathway (FDR = 2.22 E-03). **(E) G**alactose metabolism (FDR = 0.0054311). **(F)** Arginine and proline metabolism (FDR = 0.0077486). **(G)** Biosynthesis of valine, leucine, and isoleucine (FDR = 0.013182). **(H)** Degradation pathways of valine, leucine, and isoleucine (FDR = 0.013182). **(I)** Metabolism of glycine, serine, and threonine (FDR = 0.013182). **(J)** Biosynthesis of pantothenate and coenzyme A (CoA) (FDR = 0.014686). **(K)** Caffeine metabolism (FDR = 0.002563). Identified (based on MS/MS) and tentatively labeled (based on comparison of accurate m/z and database) metabolites are shown in red font.

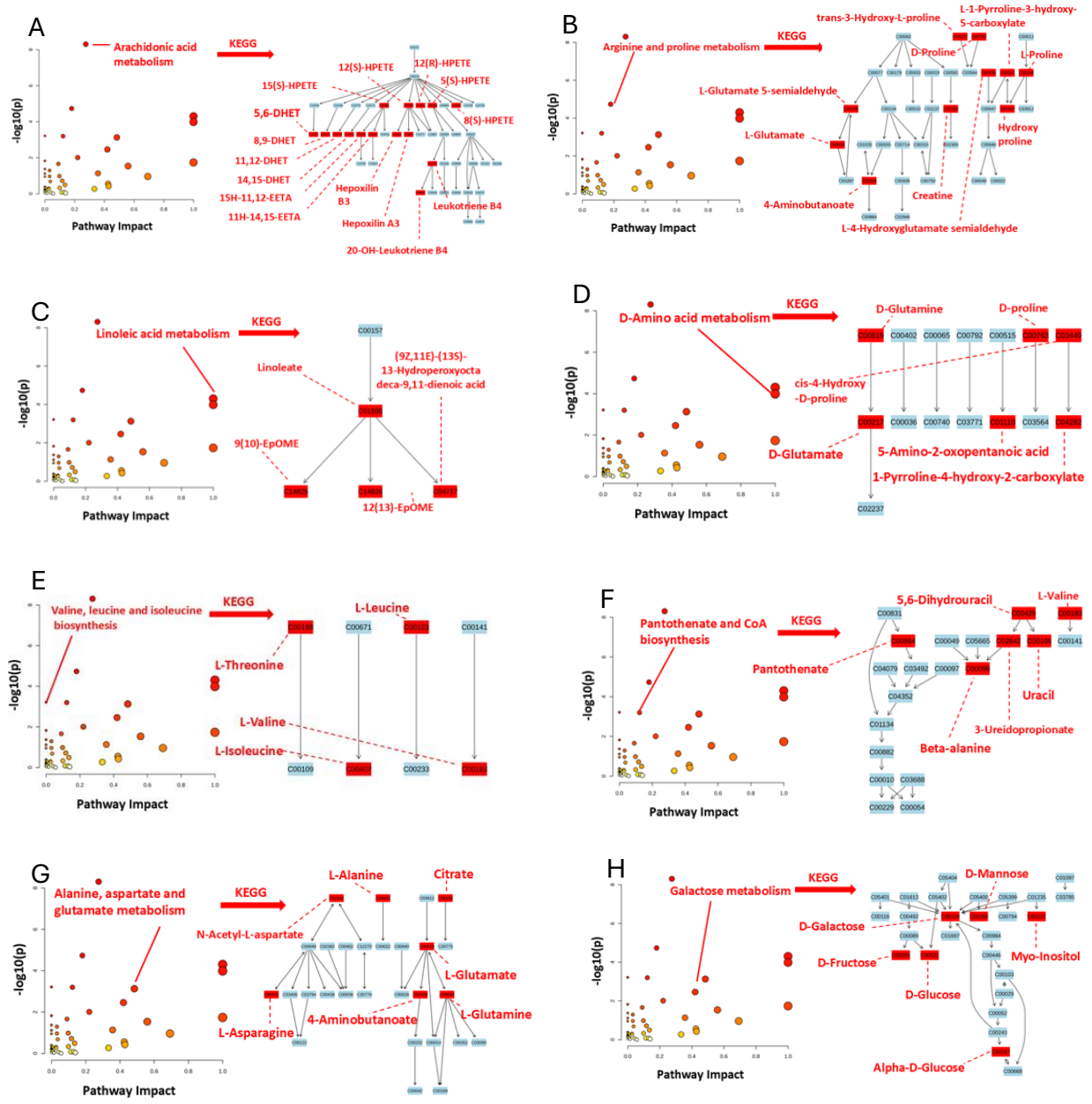

Figure S10. Pathway analysis using significantly changed metabolites ($p<0.05$ and FC > 1.5) from the comparison between Group 1 and Group 3 in the negative ion mode. **(A)** Arachidonic acid metabolism (FDR = 3.96×10^{-7}). **(B)** Arginine and proline metabolism (FDR = 7.40×10^{-4}). **(C)** Linoleic acid metabolism (FDR = 1.33×10^{-3}). **(D)** D-Amino acid metabolism (FDR = 2.07×10^{-3}). **(E)** Valine, leucine and isoleucine biosynthesis (FDR = 8.45×10^{-3}). **(F)** Pantothenate and CoA biosynthesis (FDR = 8.45×10^{-3}). **(G)** Alanine, aspartate and glutamate metabolism (FDR = 8.51×10^{-3}). **(H)** Galactose metabolism (FDR = 3.48×10^{-2}). Identified (based on MS/MS) and tentatively labeled (based on comparison of accurate m/z and database) metabolites are shown in red font.

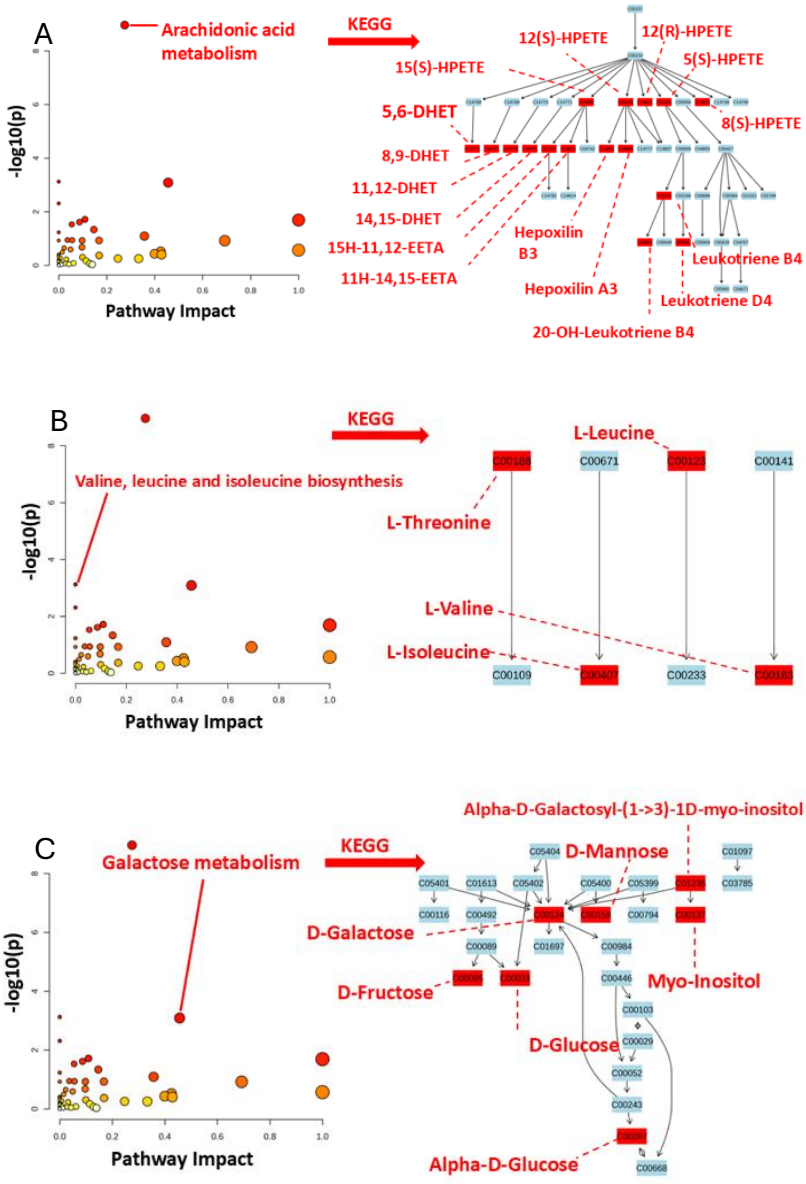

Figure S11. Pathway analysis using significantly changed metabolites ($p<0.05$ and FC > 1.5) from the comparison between Group 2 and Group 4 in the negative ion mode. **(A)** Arachidonic acid metabolism (FDR = 8.63×10^{-8}). **(B)** Valine, leucine and isoleucine biosynthesis (FDR = 2.17×10^{-2}). **(C)** Galactose metabolism (FDR = 2.17×10^{-2}). Identified (based on MS/MS) and tentatively labeled (based on comparison of accurate m/z and database) metabolites are shown in red font.